ADVANCED ENERGY MATERIALS
www.advenergymat.de

Process Parameter Specification and Control in Solution Processing of Hybrid Perovskite Photovoltaics: From Domain-Specific Jargon to Evidence-Based, Unambiguous Description of Experimental Workflows

Simon Ternes, Christoph J. Brabec, Luigi A. Castriotta, Thomas Exlager, Karen Forberich, Alessio Gagliardi, Michael Götte, Florian Mathies, Sinclair Ryley Ratnasingham, Lennart K. Reb, Eva Unger, and Aldo Di Carlo**

Within the last 20 years, hybrid perovskite solar cells (PSCs) have reached remarkable power conversion efficiencies. Further, scalability of hybrid perovskite deposition routines and stability of PSCs have been significantly improved. Yet, a critical roadblock remains: Poor reproducibility largely caused by inconsistent control and reporting of process parameters. Key aspects such as the handling of the perovskite solution, the air jet used for drying, or the process atmosphere are often incompletely specified. In response, this review systematically presents the empirical evidence linking process parameters to the film morphology and the device performance for solution-based one-step and two-step deposition routines of highly efficient PSCs as well as large-area perovskite modules. To maximize interdisciplinary understanding, the process parameters are standardized within the thin-film solar cell ontology (TFSCO), structured according to the internal logic of sequential deposition and classified by fundamental mass transfer mechanisms. In a final literature study, the state-of-the-art of parameter reporting is assessed—mirroring to the community where reporting standards can be improved. By using the here-presented parameter list as a template, perovskite workflows become fully and unambiguously specified—bridging the gap between manual and automated process optimization and fostering data-driven acceleration via digital twins of perovskite research.

1. Introduction

Since their first application in photovoltaics (PVs) ≈15 years ago,[1–4] hybrid perovskites have experienced rapidly growing research interest. The new class of defect-tolerant[5] and highly customizable semiconductors[6–8] finds application as light emitting diodes,[9–11] lasers,[6,12–14] X-ray detectors,[15–17] thermo-electrics,[18,19] transistors[20–22] and PVs.[4] In 2024, in the field of PVs alone, ≈20 new reports on hybrid perovskites were published every day on average.[23] As a remarkable result of this intense research activity, peak power conversion efficiencies (PCEs) of perovskite solar cells (PSCs) have already surpassed 27% and PSC stability has been significantly improved to thousands of hours of operation.[24–26] The quest for large-scale commercial adoption[27–34] primarily takes two forms,

S. Ternes, A. Di Carlo
Institute of Structure of Matter – National Research Council Rome (ISM-CNR)
via del Fosso del Cavaliere 100, Rome 00133, Italy
E-mail: ternes@ing.uniroma2.it; aldo.dicarlo@ism.cnr.it

S. Ternes, L. A. Castriotta, A. Di Carlo
CHOSE (Centre for Hybrid and Organic Solar Energy)
Department of Electronics Engineering
University of Rome "Tor Vergata"
via del Politecnico 1, Roma 00133, Italy

The ORCID identification number(s) for the author(s) of this article can be found under https://doi.org/10.1002/aenm.202503187

DOI: 10.1002/aenm.202503187

T. Exlager, S. R. Ratnasingham
Solar Technology and Applications (STA)
The Netherlands Organization for Applied Scientific Research (TNO)
High Tech Campus 21, Eindhoven 5656 AE, The Netherlands

M. Götte, F. Mathies, L. K. Reb, E. Unger
Helmholtz-Zentrum Berlin für Materialien und Energie
HySPRINT Innovation Lab
Kekuléstraße 5, 12489 Berlin, Germany

C. J. Brabec, K. Forberich
Department of High Throughput Methods in Photovoltaics
Forschungszentrum Jülich GmbH
Helmholtz Institute Erlangen-Nürnberg for Renewable Energy (HI ERN)
91058 Erlangen, Germany

C. J. Brabec, K. Forberich
Materials for Electronics and Energy Technology (i-MEET)
Friedrich-Alexander-Universität Erlangen-Nürnberg
91058 Erlangen, Germany

as low-cost single junction PV[35,36] or as a high-bandgap absorber for tandem solar cells with silicon.[36,37] In pilot projects, first perovskite-based PV products were delivered to assess whether a major market push within the coming years is feasible.[34,38,39] Gigawatt scale production lines have recently started production or are expected to reach operability very soon.[40] This projected market entry marks a major success of the perovskite research community who not only improved the technology within the laboratories but also disseminated it from academia into the commercial sector via spin-offs and cooperative projects.[41] In turn, the first commercial applications of hybrid perovskite PVs will further fuel academic and industrial research on the technology aimed at addressing the urgent matter of climate change.[42]

Up to the present day, academic research on perovskite PVs has placed a major focus on advancing PSC performance and stability in proof-of-principle test devices on different scales[2,43,44] ($1mm^2$ – $1m^2$). For the solution processing methods discussed in this review, significant advances were achieved by improving processing methods,[45–47] the perovskite composition[48–50] and structure,[51,52] the solvent system,[53–56] charge transport layers,[57,58] passivation agents as well as interlayers[59–61] and additives.[62–64] As alluded to before, a major part of this technological development has already been passed on to industry or projects with substantial industrial involvement.[41] Due to the large commercial interest, a shift of research focus, from single performance indicators such as PCE or stability, toward high technology readiness levels, adapting combinations of performance indicators, is soon to be expected.[65] Thus, with industry doing the heavy lifting of technological development, publicly-funded research has the privilege to tackle the remaining challenges. These are fundamental barriers to the technological readiness of perovskite PVs that could hinder their large-scale roll-out in the future. Main challenges arise from limitations of (i) module and cell durability, (ii) PCEs at scale and (iii) production yield during manufacturing.[66,67] This review presents an overview of literature addressing challenge (iii) by focusing on specification of process parameters of perovskite solution processes. It further showcases concrete guidelines of how these parameters can be controlled in the laboratory. To manage the extent of the analysis, we restrict this review on solution processing methods. A similar analysis of process parameters can and should be conducted for dry deposition processes such as thermal evaporation and sputtering in the future. We further like to stress the enormous value of rigorous and standardized characterization of perovskite morphology and functionality of PSCs by means of microscopy, spectroscopy and standardized opto-electronic measurements. However, while there are numerous, excellent works and reviews on the characterization of PSCs and perovskite films,[68–73] the input variables of solution processes for perovskite thin film fabrication have never been summarized in an exhaustive overview.

In practice, most academic research on PSC fabrication is guided by intuitive trial-and-error manufacturing of spin-coated PSCs, where the "art of device making" is passed from one generation of researchers to the next.[74] This practice is very advantageous: it is a representation of rapid prototyping,[75] where new material combinations and processing steps can be rapidly tested and optimized. The result is a steep improvement in device performance and reliability within every participating laboratory. However, each laboratory has its own version of the reported processes and, in many cases, its own laboratory jargon adapted to its present toolset and materials. To make matters worse, there is no explicit consensus in the community as to which process parameters need to be reported for a perovskite process to be reproducible.[76] As a consequence of the above-described inconsistency and incompleteness in reporting, in practice, perovskite solution processing is challenging to transfer from one laboratory to another. For example, differences in the handling of the antisolvent treatment step in PSC device fabrication are often not clearly specified. These differences concern process parameters such as the pipette tip diameter, the distance from the sample or the rate of solvent ejection. Similarly, there are often incompletely specified drying processes, missing information on the distance of the gas nozzle, the nozzle diameter and the rate of gas purged from the nozzle. Another potential consequence of inconsistent vocabulary and incomplete specification is the difficulty of interdisciplinary cooperation. For example, the term "quenching" frequently used in the sense of a processing step within the field of perovskite PV (as in this work) is hard to understand for researchers not specialized within the field.[77]

With the widespread industrial adoption of perovskite research, the time has come to decisively address the persistent problem of inconsistent and incomplete reporting. To ensure reproducibility and accelerate progress, the research community must find common ground on standardization of all workflow steps and parameters involved in the fabrication of PSCs. This requires. 1) A precise and exhaustive classification of the fundamental workflow steps involved in perovskite deposition. 2) A clear specification of all critical process parameters that must be monitored and controlled within each step to guarantee standardized and reproducible experimental conditions. 3) A detailed, practical definition of how each process parameter is to be adjusted, measured, or documented in real-world laboratory and industrial settings. In this regard, an analogy to the characterization of perovskite device performance and stability can be drawn, where rigorous design of standard measurement conditions leads to an enhanced reliability and comparability of the obtained results.[68,72,78,79]

When standardizing perovskite process parameters, the complexity of a modern day laboratory involving numerous tools, processes and parameters as well as their interrelation can become a challenge. If standardization is defined by text in human language, this complexity will manifest in lengthy, repetitive paragraphs prone for misunderstanding. A much better approach of standardizing workflows is the digital representation

C. J. Brabec, K. Forberich
Photovoltaics (IMD-3)
Forschungszentrum Jülich
Wilhelm-Johnen-Straße, 52428 Jülich, Germany
A. Gagliardi
Department of Electrical Engineering
TUM School of Computation
Information and Technology
Atomistic Modeling Center (AMC)
Munich Data Science Institute (MDSI)
Technical University of Munich
Hans-Piloty-Straße 1, 85748 Garching, Germany

of these real-world objects, their properties and interrelations in a so-called process ontology capturing and defining all domain-specific terminology in a systematic way.[80] Developing and employing such ontology is a first step toward digital laboratory management tools and digital twins that can be broadly adopted across the research community. These digital twins synergistically benefit from automation of processing equipment[81–84] and in situ characterization.[56, 85–88] For example, measurements of thin film thickness during spin coating can be used as process triggers, enhancing process control as well as the reproducibility of the final films.[89] Another route is the optimization of process parameters via their photoluminescence as a quality indicator.[82,87,88,90,91] While these are exemplary demonstrations of high-control reactive environments, the vast majority of work groups may not have these sophisticated tools at their disposal. This is where the parameter table presented in this work, referenced to the thin-film solar cell ontology (TFSCO), can help in closing the gap between highly automated and manual laboratory routines.[80] TFSCO mirrors the internal logic of perovskite solution deposition according to the principle "Putting-things-on-top-of-other-things", where a sample or "state" is streamlined through a timely sequence of workflow steps modifying the sample (or "state"). Each workflow step is defined by a fixed set of process parameters. To maximize standardization, the designation and logical structure of these steps are harmonized within the ontology and made accessible via Uniform Resource Identifiers (URIs).[92] In this way, the specification gap between automated and manual device optimization can be effectively addressed and the implementation of digital twins is greatly facilitated.[93]

While the issue about "hidden variables" for reproducing perovskite solution processes has been touched upon before,[76] there is currently no conclusive summary of all important variables in perovskite solution processing to our knowledge. This is astonishing given that the importance of standardization of measurement conditions was pointed out early on.[68] We are convinced that the ability of reproducing PSC fabrication in different laboratories should at least obtain the same attention. In response, we see this review as the first opportunity for perovskite researchers to obtain a conclusive and logically structured list of all relevant workflow steps for solution processing and their respective process parameters as evidenced by state-of-the-art literature.[94] Especially for researchers or technologists new to the field, this review serves as a good starting point, detailing on how to control and report perovskite solution processes in a reproducible manner. Also experienced researchers can find merit in the logically structured parameter list accompanied by explicit guidelines. The reason is that full parameter specification, standardization of process description and vocabulary enhance not only reproducibility of processes, but also reusability and impact of the published data. Adherence to these standards will greatly facilitate the (semi-)automatic creation of databases according to Findable, Accessible, Interoperable and Reusable (FAIR) principles.[95,96] In practice, scientific data management software systems are used to organize and structure the massive amounts of experimental data generated in modern laboratories.[97] Relying on one of these systems, the present review and the updated TFSCO, researchers can easily label and publish datasets that can be exploited for training machine learning algorithms, later on. These algorithms provide data-driven insights beyond human intuition and trial-and-error optimization. Certainly, there is no such thing as perfect reproducibility of processes due to (practically) uncontrollable variables and inherent process variances. However, adhering to the here-discussed standard can be a crucial step to identifying the fundamental limitations of reproducibility of perovskite solution processes. Such high-quality data on process capability will be invaluable for consistent industrial manufacturing on commercial scales.

This review is structured as follows: In section "2. Perovskite Solution Deposition" we revisit the historical development and terminology of PSC solution processing in the light of mass transfer dynamics, which may provide an interesting new perspective to many readers. In section "3. Pivotal process parameters impacting perovskite solution processing" a check list of decisive process parameters is presented. In this section, we lay the foundation for establishing a standard description for PSC fabrication routines by summarizing state-of-the-art evidence on the impact of process parameters on two-step and one-step processing. In **Table 1**, we provide concrete guidelines of how control and/or measurement of each parameter can be implemented in the laboratory. Eventually, in section "4 Current Literature" we present a mini survey on the status of reporting of process parameters in state-of-the-art literature and conclude with section "5 Conclusion and Outlook", where we present the next steps and open questions for standardization of perovskite solution processes.

2. Perovskite Solution Deposition

From the outset 20 years ago, research on hybrid perovskites for PVs led to two principal routes of perovskite deposition emerging: Deposition from the vapor phase[98] and the liquid phase.[99] More recently, the two deposition strategies are combined in the so-called hybrid approach.[99] In this review, we primarily focus on the solution processing route. This route was applied for the first time when introducing perovskite as possible dye sensitizers to a mesoporous scaffold of titanium dioxide as an electron transport layer.[100,101] While mesoporous perovskite devices are still developed further, both the n-i-p and the p-i-n planar device architectures have become very popular for high-PCE devices.[2,102] Solution processing splits further into two subclasses: 1) Processing from one solution containing all necessary precursor chemicals for completing the perovskite stoichiometry ABX_3, often accompanied by so-called quenching methods and 2) sequential layer or 'two-step' deposition: A film of BX_2 salt(s) is coated, which is subsequently brought in contact with an AX solution (film).[103] Both processing routes are engineered to address the critical challenge of controlling perovskite crystallization kinetics—ensuring homogeneous film formation, appropriate grain size, and controlled thickness across large areas.[104] In more practical terms, they answer the question of how to deposit a homogeneous, substrate-covering layer of a (poly)crystalline material that exhibits a well-defined thickness in the range 0.3-1.5 µm. While conceptionally different, the two routes still follow the same logical structure, which we denominate as "Putting-things-on-top-of-other-things". This is to say that, in the workflow, a sample is passed on from one workflow step to the next in a timely succession with possible intermediate time delays as shown in **Figure 1**. In the following, we introduce the one-step deposition of

Table 1. Overview of Parameters, units, typical ranges, and best practices/control setups in perovskite solution processing as a complement to Figure 1. In practice, the Excel sheet in the supplementary is ready to be used for reporting of parameters. Some best practices are marked (rec. = recommended), which means that they are not required to reproduce a process, but provide a higher degree of details. To maximize standardization, all of the depicted parameters were included in the TFSCO systematized according to the quenching techniques and associated with an appropriate URI (see Table S2, Supporting Information and ref. [80]). For evidence in support of the choice of the concrete process parameters, see corresponding subheading in Sections 3.1–3.4.

		Parameter	Units	Typical range	Best practice/Setup for control
General		Composition of atmosphere	%w, ppm, ppb	20 g/m^3 H_2O – 1ppb H_2O, 21% O_2 – 1 ppb O_2	• Report type of atmosphere, • Measure humidity in ambient atmosphere, • Report ppm/ppb of trace gases in gloveboxes • Report on the purity of the air in cleanrooms • Limit solvent usage/report amounts and frequency of solvents used as well as used solvent filters (be aware of the difference between relative humidity and absolute per cent of water molecules)
		Pressure of atmosphere	Bar, Pa, atm	1 atm, 10^5 – 10 Pa	• Measure when quenching at reducing pressure
		Temperature of atmosphere	°C, K	15–80 °C	• Use a thermometer in the processing environment
		Solution Composition	ml, µL, mmol,	5–0.1 mmol, 10mL–1 µL	• Use Excel sheet from[76] for exactly specifying amounts and suppliers of chemicals
		Solution handling	–	–	• Specify whether the solution was stirred and how long (if so provide details about the used device), in which order the precursors were added and if elevated temperatures were used • (Rec.) Record a video of the preparation of solution
		Solution resting time	h, min, weeks	10 min – 10 weeks	• Report (incl. stirring if used)
		Substrate Type	–	–	• Report the substrate material (glass, PET, PVT) and thickness but also the supplier • If available, report surface profilometry measurements or similar characterization methods on pristine substrates
		Substrate Handling			• Report how the substrates are cleaned • (Rec.) photo of cleaning process • (Rec.) provide details on the substrate holder during deposition
		Substrate dimension / Area of Interest	cm × cm	(1 cm – 300 cm)^2	• Report dimensions • Take photo with reference scale • Indicate area of interest (e.g. active area)
		Substrate movement	cm/s, rpm	100 –0 cm s^{-1}, 100–10.000 rpm	• Report • (Rec.) Record video with reference scale
		Substrate temperature	°C, K	15–200°C	• Report temperature setpoint • Report model of hotplate and placement of samples • (Rec.) Infrared picture of hotplate temperature distribution and/or on samples
		Previously deposited layer/Contact angle	(°)	1°–80°	• Report parameters of previous layer deposition • If used, report steps of substrate activating processes • Measure contact angle of perovskite ink
		Deposited wet film thickness	µm	1–5 µm	• Report coating parameters fully specifying the used coating technique • Calculate wet film thickness from measurement of dry film thickness
		Time to next step	Min, h, weeks	10min – 10 weeks	• Report
One step	All (except rad./thermal)	Quenching medium	–	Dry Air, N_2, antisolvent	• Report exact composition of quenching medium • If quenching with gas, use the same gas as the surrounding gas • If working in glovebox, limit concentration of solvent vapor and ensure proper circulation and cleaning
	Impinging jet	Nozzle geometry and size	mm, µm	0.01–10 mm	• Report • Provide geometry (round nozzle, slot nozzle are common standards), provide a sketch if non-standard geometries are used

(*Continued*)

Table 1. (Continued)

		Parameter	Units	Typical range	Best practice/Setup for control
		Nozzle output velocity or flow rate	m/s (µL/s)	0.01–200 m s^{-1}	• For gas quenching, measure with a mass flow controller • For antisolvent quenching, provide a video • (Rec.) use an electronic pipette with rate control
		Nozzle distance from sample	mm	0.1–50 mm	• Use a well-defined distance fixed by a mechanical mount or, alternatively, record a video with a scale in the background
		Impingement angle	°	10°–90°	• Use a well-defined angle by a mechanical mount or, alternatively, record a video
	linear flow	Flow geometry	mm, cm, etc.	10cm x 10cm – 100cm x 100cm	• Exactly specify the dimensions of the chamber, the connections to the inlet and outlet, the pump model (if used) and the location of the sample • (Rec.) Provide a CAD drawing of vacuum chamber
		Flow velocity	m/s	0.01–10 m s^{-1}	• If a pump is used: Provide the pump model and its volumetric extraction rate as a function of pressure • For high enough pressures: Measure the velocity with a mass flow controller or an anemometer (Alternatively, perform flow simulation) • Exactly specify, which valves are used and at which moment they are opened • Record a video of the process
		Pressure of Atmosphere	Pa, bar, atm	10^5–10 Pa	• Measure static pressure at multiple positions in the chamber as a function of time if it deviates more than 10% from atmospheric pressure at sea level
	Natural/diffusive drying	Geometry of room/vessel and disturbances	mm, cm, m, etc.	–	• Record a video of how and where the sample is dried / immersed • For natural drying: Measure relative air speed over the sample with an anemometer • For antisolvent, try to visualize the flow field for example by introducing suspended particles • Show how the drying process is influenced by intentional disturbances. These can be a fan for natural drying or stirring for antisolvent
	Radiative/thermal	Radiation type	–	–	• Provide type of radiation, such as plasma or temperature conduction
		Geometry radiator/hotplate	mm, cm, m, etc.	–	• Provide supplier and model of tool (IR annealer, hotplate) • (Rec.) provide a CAD drawing
		Rad. Intensity/ heat flux	W, kW	–	• Provide an estimate for the intensity or power of the provided radiation / heat flux • Alternatively, measure the temperature change of the sample when the annealing process is started over time
		Distance from sample	cm, mm, µm	–	• Report • If the sample is placed directly on the radiation/heat source, estimate the distance by measuring the roughness of the sample and/or the temperature distribution on the sample as described above
		Irradiation/heating time	Min, s	–	• Report
Two-step		Cation Solution Composition	ml, µL, mmol,	5–0.1 mmol, 10mL–1 µL	• Use Excel sheet from[76] for exactly specifying amounts and suppliers of chemicals
	Init. Annealing	Annealing time / Drying time	min	1s – 60 min	• Report (annealing is optional, however if no annealing is used, the time between the first and second step is crucial)
		Annealing temperature	°C, K	20–80°C	• Report (if annealing used)
		Annealing/Drying atmosphere	%w, ppm, ppb	20 g/m^3 H_2O -1ppb H_2O, 21% O_2 – 1 ppb O_2	• Report as described above if different from atmosphere of first step application (be aware of the difference between relative humidity and absolute per cent of water molecules)
	Coating	Wet film thickness / Deposition parameters	–	–	See above

(*Continued*)

Table 1. (Continued)

		Parameter	Units	Typical range	Best practice/Setup for control
		Drying / Quenching parameters	–	–	See above
	Immersion	Vessel geometry	mm, cm, etc.	10cm x 10cm – 100cm x 100cm	• Provide a model/drawing/photograph with a references such that absolute dimensions are visible of the used beaker/vessel
		Immersion/Stirring	descr., rpm	10–100 rpm, stirrer	• Record video of process of dipping/stirring/moving the sample through the cation solution
		Reaction time	min	0.1–60 min	• Report
Final		Time until annealing	min/h	0.01–10 min	• Report
		Annealing time	min/h	0.1–100 min	• Report
		Annealing temperature	°C, K	30°–200°	• Report • (Rec.) Infrared camera photo / movie of temperature distribution on the hotplate • If the sample is placed directly on the hotplate, estimate the air gap by measuring the roughness of the sample. In ideal case, use a well defined air gap.
		Annealing atmosphere	%w	0–30% humid., 21% O2 – 1 ppm O2	• Report if different from processing atmosphere

perovskite thin film from solution in detail – structured according to the specific, available quenching methods (Section 2.1) – and conclude by detailing two-step procedures (Section 2.2) and outlining their similarities with the one-step processing methods described before.

2.1. One-Step Deposition of Perovskite Absorber Thin Films

2.1.1. Historical Origin of the Term "Quenching"

To date, one-step deposition procedures are the most common method to fabricate perovskite absorber films from solution.[105] These methods usually require a so-called "quenching step" to induce the nucleation of halide perovskites in a controlled manner. For large-scale perovskite deposition, one-step processing is used even more frequently.[44] The origin of the term 'quenching' is in the field of metallurgy, where it describes the rapid cooling of a hot metal piece, potentially preventing undesired phase-transitions.[106,107] To our knowledge, the first occurrence of the term 'quenching' within the field of perovskite PVs (meant in the sense of a processing step) is dated to January 2015: Hwang *et al.* reported on large-scale PSCs by a two-step fabrication method of slot-die coated PbI_2 that was subsequently dipped in methylammonium iodide (MAI) solution.[108] In this report, they described the process of using a slot nozzle purged with nitrogen to dry the deposited PbI_2 solution film as "Gas-quenching" (the quotation marks are also present in the original publication, hinting at a rather colloquial use of the term). Contrary to its original meaning, it is, however very unlikely that the cooling effect of the forced convection played a major role in the morphology formation of the PbI_2. Instead, it is believed that the difference in the morphology formation of PbI_2 was induced by rapid drying due to the impinging air jet.[109–111] As of today, 'quenching' as a general process description spread throughout the whole perovskite research community. Beyond the still commonly applied gas quenching, the terms 'antisolvent quenching' and 'vacuum(-assisted) quenching' were introduced as domain-specific laboratory jargon. Notably, these terms are not to be confused with quenching of luminescence[112] discussed in opto-electronic devices. It is therefore a valid option to replace the term "quenching" with "drying" or at least to mention "drying" alongside in publications, as the latter is more general and easier to understand outside of the field.

2.1.2. Precise Definition of Quenching

When the general term 'quenching' is used in conversations within the field of hybrid perovskite thin films, researchers refer to the processes of quickly supersaturating the solution film. The intention is that a high density of closely spaced crystal seeds are created within a short time to confine the space for subsequent crystal growth.[113–115] As shown before, mass transfer plays a crucial role in achieving a high enough supersaturation increase[116] at exactly the moment, when the solution reaches critical concentration for crystallization.[104,117] In detail, we would like to define quenching herein as the aggregative term of three well-defined sub-processes:

I. Mass and/or heat transfer between the film with the environment due to a specific action such as release of antisolvent or opening of a gas nozzle
II. Change of the concentration and/or chemical environment of the dissolved/complexed precursor solution film due to (i)
III. Morphology transformation (involving drying, crystallization, agglomeration, etc.) within the thin film induced by (ii)

In the above sense, quenching designates both the processes of rapid drying and/or diffusion through the film surface as well as the simultaneous crystallization from solution as induced by a rapid supersaturation increase.[104] We note that heat transfer may play an important role in quenching,[118–123] but this is not

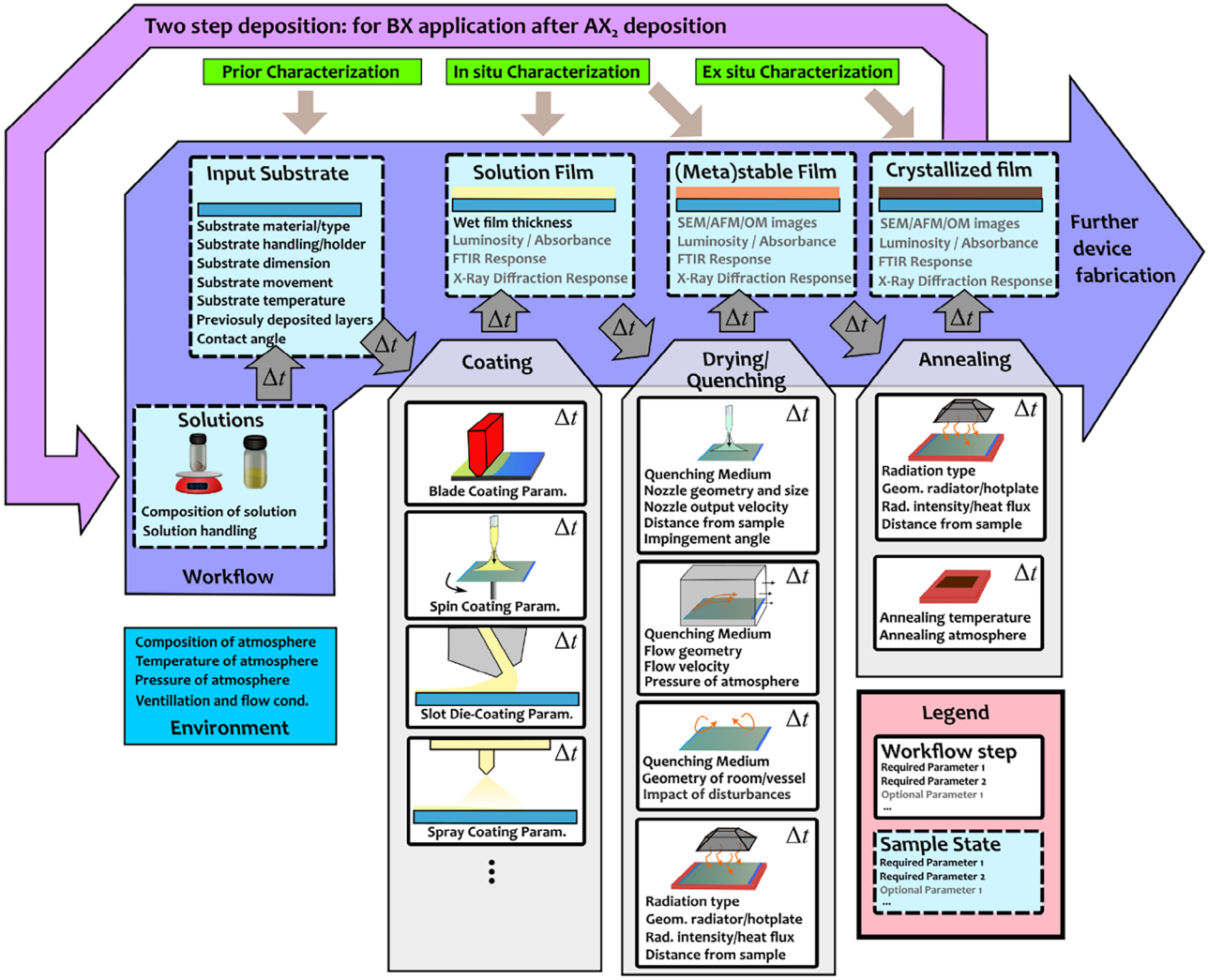

Figure 1. Process parameters involved in perovskite solution processing are structured into states (light blue boxes with dashed borders) and workflow steps (gray boxes with solid borders). Required parameters for specification of workflow steps are drawn in black, while optional parameters that can be measured for additional insight are drawn in gray. The logical succession of states through modification by workflow steps according to the "Putting-things-on-top-of-other-things" logic is conceptualized by the purple arrow with the label "workflow", where some parameters of the environment are kept constant (blue box). The general idea is that a (semi)stable state is passed on from one step in the workflow to the next in a timely succession, where the choice and order of the latter completes a deposition workflow. According to this logic, two-step processes may be represented by a recurrent loop within the workflow symbolized by the thin arrow on top (which means that all depicted parameters involved in the first step need be specified again). The gray arrows with the label Δt indicate that time differences between the execution of the process steps should be known and the Δt symbols in the top right corner of the steps indicate that every step has an intrinsic duration, as well. Opportunities for characterization are shown in green boxes. Characterization is paramount for tackling remaining drifts in material systems and surveilling the quality of the perovskite deposition process.

always the case (for example, if the film is kept at a constant temperature and potential evaporative cooling is balanced instantly by a heat conduction). In contrast, mass transfer with the environment is present within all quenching processes (to our knowledge, there is only one exception of perovskite crystallization from molten salt liquids without mass transfer,[124] which is however not widely adopted). Using the above definition, it is sensible to distinguish quenching further by the involved mass transport mechanisms (see tab "Drying/Quenching" in Figure 1). Correct specification of mass transport[125] dictates which process parameters are required for the respective quenching methods constituting blocks in Figure 1.

2.1.3. Impinging Jet Quenching Using Antisolvent or Gases

Here, an impinging jet of either a gas or an antisolvent is established on top of the perovskite solution film to extract the solvent from the film and/or exchange the solvent in the film by an antisolvent. Impinging jet quenching using antisolvent was historically the first quenching method used for inducing perovskite crystallization.[45,126] Until now, antisolvent quenching (also referred to as "antisolvent treatment" or "solvent engineering" method) remains the most common way of fabricating perovskite absorber layers in literature, and in particular, for fabricating world-record PSCs.[102] One of the reasons is that

antisolvent quenching is very effective due to the high supersaturation rates induced by liquid–liquid mass transfer.[104] However, this methodology is not commonly used in works on large-scale perovskite deposition (with some exceptions),[127–129] where gas quenching with a slot nozzle or vacuum-assisted quenching is often preferred.[44] While the latter method does not fall under the category of impinging jet quenching (see next section), the former method is another representation of an impinging jet and involves therefore very similar process parameters. The advantages of using a slot nozzle with pressurized air is its simple setup and operation using abundantly available pressurized air lines. This simplicity reduces the potential cost for industrial production.[47,130] However, a major drawback of impinging jet quenching remains: It is difficult to obtain reproducible and homogeneous process conditions on large scale substrates due to the inhomogeneous mass transfer induced by an impinging jet.[117] For quenching using a gas nozzle, this issue can be partially mitigated by tilting the nozzle and tuning the movement of the substrate in a suitable way. However, this can still be challenging to implement in practice – in particular for batch-to-batch coating where the drying of the initial part of the substate experiences different starting conditions than the end of the substrate.[131]

2.1.4. (Vacuum Pump-Assisted) Linear Flow Quenching

Under the category of linear flow, we understand a setup in which air flows linearly over a substrate along a pre-defined direction, where the dimensionless Reynolds number[132] is decisive for the build up of either turbulent or laminar flow.[125] As opposed to impinging jet quenching discussed before, the employed fluid does not directly impinge onto the sample but steadily flows over the sample. Although treated by some groups previously,[133,134] it might seem that linear flows would not find an extensive application in the field of perovskite PV. However, vacuum-assisted quenching methods, which have become very popular for the fabrication of high-quality and scalable batch-to-batch processed perovskite PV,[135–142] ressemble linear flow quenching methods.[104] In detail, a vacuum pump induces an air flow alongside an exponential decrease of pressure, increasing mass transfer into the gas phase, which, in turn, helps to supersaturate the solution rapidly.[104] Possibly the biggest advantage of this method is that the mass transfer is rather homogeneous on a lateral scale as compared to the impinging jet, greatly facilitating its scalability for batch-to-batch operation.[143] Similarly, a substrate that is moved through an antisolvent bath or is coated with an antisolvent will be subject to a net linear flow of antisolvent.[127,129,144]

2.1.5. Natural Drying and Convective/Diffusive Quenching

When a film dries naturally or a film is immersed in a large volume of antisolvent, convective or diffusive mass transfer (or a combination of the latter) is apparent[145,146] (colloquially, some perovskite researchers would not designate natural drying as a quenching process, but the above definition can still be applied). Diffusion occurs due to the Brownian motion of molecules. At the same time, convective eddies may build up due to differences in buoyancy of fluid close to the film as compared to the surrounding fluid (this can also be a negative buoyancy due to solvent molecules from the perovskite film having a higher density than the surrounding medium).[147] An antisolvent bath acts analogously to natural drying: The only particle transfer is caused by diffusion due to Brownian motion and, potentially, natural convection induced by the different buoyancy of the liquid close to the film (neglecting for a moment the fact that the process of substrate immersion induces a flow of antisolvent over the substrate). A clear advantage of natural drying for industrial feasibility is the simplicity of the process requiring no additional processing equipment (except proper ventilation and potentially recycling of solvent vapor). It is therefore very cost-effective for industrial-scale application.[148] However, one of the downsides is that little changes in environmental ventilation or the sample transport can induce distortions in the convection over the substrate. These changes may alter the drying dynamics and impact product yield.[146] Since movement of air is always present in a real-world fabrication environment, this type of drying might be challenging to reproduce. A similar consideration applies for the antisolvent bath, where the sample transfer certainly induces a complex fluid flow that impacts mass transfer.

2.1.6. Radiation/Plasma/Heat Induced Quenching

Some quenching methods cannot be classified into either of the above categories. For example, the perovskite solution film can be exposed to a flux of photons (mostly infrared radiation),[119,122,123,149,150] a plasma[151] or a rapid heat conduction through the substrate.[118,120,121] The advantage of these methods is that they are compatible with high-throughput processing. They further allow for the reduction of process complexity by combining quenching and annealing in a single process step. However, due to the rapid dynamics involved, it is difficult to identify cause-and-effect relationships for these techniques correctly. For example, when using infrared radiation, the film heats up rapidly, in turn, experiences accelerated evaporation of solvent out of the film and accelerated crystal growth. It is therefore very hard to predict which morphology forms as fast evaporation leads to homogenized morphology, while extensive crystal growth can create large crystallites with gaps of low substrate coverage.[115,117] For heat-induced quenching, heat conduction through the bottom surface dictates the morphology formation. The dynamic temperature change and stabilized temperature distribution on a substrate can be difficult to quantify due the complexity of modelling heat transfer through the substrate. An accurate model would include the inhomogeneous air gap spacing between the substrate and hotplate and the lateral temperature distribution of the hotplate. Therefore, thermal cameras and/or temperature sensors should be employed when using these techniques.[152–154]

2.1.7. Combining Different Quenching Methods

Lastly, we would like to stress that multiple quenching methods can be combined.[122,127,129,144] For example, gas quenching can be employed to pre-dry the perovskite solution film and then the perovskite nucleation can be induced by antisolvent quenching or infrared radiation. In the case where multiple quenching

methods are combined, the process parameters for each individual method, as detailed below, must be specified.

2.2. Two-Step Deposition of Perovskite Absorber Thin Films

The second principal route for fabricating perovskite absorber films is the so-called sequential deposition or two-step route.[103,155] A layer of a pure lead halide salt (or a mixture of these) is deposited independently from solution, or alternatively vapor-deposited, in a first step. Subsequently, in a second step, a film of a cation solution is deposited by a common solution deposition technique or alternatively, from a bath[156,157] or a vapor[158,159] (in case vapor and solution steps are combined the process is referred to as hybrid).[160] The film is then annealed to induce/complete the conversion of the sequential films to form a halide perovskite film. Although two-step deposition of perovskite thin films is less often used in large-scale device fabrication (with notable exceptions),[122,158,161,162] it has become a popular alternative for fabricating high-PCE devices[102] and tandem devices.[163,164] In contrast to one-step deposition, the perovskite morphology formation is controlled by the coating of the cation layer and the subsequent conversion to perovskite. It was shown that for two-step deposited perovskite films, the porosity and/or roughness of the lead iodide film has a crucial impact on the thin film quality.[165–168] As already mentioned above, to control the morphology of the first step, similar quenching methods can be applied as in one step processing.[169,170] Conceptionally, the coating of a second layer on top of the BX_2 layer can be seen as a replicate of the first coating step (such that a new instance of the same parameters according to the chosen workflow steps apply). However, it must be considered that two-step deposition is a more complex process involving simultaneous mass transfer and diffusion of a multicomponent system, intercalation and phase transitions.[171] We will, nevertheless, take advantage of the similarities between the one-step perovskite deposition and the application of either step during two-step deposition, concluding that, in principle, similar drying and/or quenching methods can be used (see recurrent arrow in the flow logic of Figure 1). In the conclusive analysis in section 4, we will further illustrate that the outcome of the second step application not only depends on its process parameters but also on the (possibly transient) properties of the states passed on from the processing of the first step. Spectroscopic or microscopic characterization of this intermediate state is therefore highly recommended.

3. Pivotal Process Parameters Impacting Perovskite Solution Processing

In this section, we summarize state-of-the-art evidence on the impact of individual process parameters on the perovskite morphology formation within one- and two-step processing building on the logic introduced in Figure 1. *A process parameter is, in our view, a physical quantity that can be measured in principle*. This definition is compatible with the fact that many process parameters are not directly measured during the workflow, most commonly if the operator trusts a prior calibration of the employed tool, for example the set rotations per minute of a spin coater or the volume scale of a pipette. We further note that this definition does not request that process parameters are always fully controllable. The distinction between controllable and non-controllable (environmental) parameters is often blurred. As an example, the laboratory humidity or temperature can be adjusted via air conditioning, but only within certain limits.

To summarize the above results and maximize their relevance to the community, we have composed a table listing all required parameters along with their typical units and value ranges (see Table 1; we summarized some ambiguous terminology of similar process and parameters in Table S1 (Supporting Information) that can be useful to understand Table 1). In the next section, we provide the detailed evidence outlining the relevance of every single parameter for improving reproducibility and quality output of perovskite fabrication routines. For each parameter, we include a recommendation as to how this parameter can be controlled and reported properly. For parameters that can be controlled in a straightforward manner, we just filled this cell with the remark "report". In a supplementary, ready-to-use Excel Sheet, we map Table 1 to the URIs of the updated TFSCO[80] to standardize vocabulary and increase machine readability (the original structure of TFSCO is depicted in Table S2, Supporting Information). We recommend the use of the Excel sheet for making sure that every required parameter of Table 1 for the respective processing method is published. Such reporting check-lists could be requested by journals in the future for the benefit of the research community. In this way, not only a quick overview is available for future experimentalists, but also machine readability according to FAIR data principles is improved tremendously. Note that the transition and use of research data management platforms such as NOMAD will facilitate adherence to harmonized and standardized reporting on sample/device preparation procedures.

Before analyzing the individual parameters, we start by specifying the process parameters that are applicable to perovskite solution processing in general during coating (Section 3.1). We then continue with one-step deposition (Section 3.2), listing the parameters for each individual quenching route, and conclude with two-step deposition (Section 3.3). The quenching methods are distinguished according to the involved mass transfer dynamics as introduced before: Impinging jet quenching using antisolvent or gas (Subsection 3.2.1), linear flow quenching (Subsection 3.2.2), natural drying or convective/diffusive (Subsection 3.2.3), and radiation/thermal based quenching (Section 3.2.4). In Section 3.4, we conclude with the process parameters that need to be specified after the coating process.

3.1. General Parameters

We start with the general parameters that must be specified for every perovskite deposition from solution (see process logic in Figure 1 and parameter list in Table 1).

Composition of Atmosphere: The composition of the atmosphere is defined by its oxygen content (% or ppm),[172–175] the humidity (RH: % or ppm, AH: g/m^3)[176–182] as well as the possible accumulation of solvent vapor in the atmosphere,[183–185] the latter being crucial for closed glovebox systems.[186] In some instances, the atmosphere is intentionally enriched with solvent

vapor to influence with perovskite morphology formation.[183,187] For these instances, it is of great help to quantify the amount of added solvent vapor and the volume of the vessel confining the atmosphere. The choice of quenching medium, described below, can have a tangible effect by superseding the present atmosphere (especially in the case a liquid antisolvent is used). However, the possibility of modification of the film surface (or the drying of the same film) before the onset of quenching due to the atmosphere cannot be ruled out. Another important aspect is the purity of the atmosphere. If for example, a cleanroom atmosphere is present, the particles per volume can be specified. If the atmosphere is (partially) ionized under conditions of intense UV light, this aspect should be studied or ruled out by systematic investigation.

Pressure of Atmosphere: Most experimental routines are performed approximately under atmospheric pressure (weather related pressure differences, pressures of impinging gas jets and altitudes above sea level should not lead to significant deviation above 10%). However, whenever significant pressure differences exceeding ≈0.1 bar are present, they should be reported. While absolute static pressure has no influence on the partial vapor pressure of solvents themselves (which are, in ideal gases, independent of total pressure), air flows at reduced pressure may allow for accelerated mass transfer during drying. The reason is that, as demonstrated before,[104] the Sherwood correlations dictating mass transfer in air flows indirectly depend on static pressure[147,188] through parameters as the Reynolds number, gas viscosity and diffusion coefficients[188] (for more details see ref. [104]). This effect is leveraged in vacuum-assisted quenching, where the surrounding pressure decreases with time.[104]

Temperature of Atmosphere: The temperature of the atmosphere severely affects the perovskite morphology formation.[189] In particular, the composition of the perovskite solution is affected by the evaporation of solvents and other volatile components into the gas phase that depends on temperature.[188] The reason is that diffusion coefficients as well as other properties such as viscosity and density of the gas are temperature-dependent.[188] Further, as alluded to above, if the temperature of the atmosphere differs from the substrate temperature, the substrate can gradually heat up or cool down. This occurs more likely if temperature differences are substantial or when the substrate is (close to) being thermally isolated (such as is the case for floating substrates or substrates on top a rubber ring employed in spin coating). Furthermore, large temperature gradients can induce convective eddies that alter film drying.[147]

Composition of Solution: One of the most important parameters that needs to be defined is the composition of the perovskite solution. If the used solution is ill-specified, the reproducibility of the process will be at risk, independent of the question of how well the following parameters are described. The main proportions of the solvents, their purity as well the suppliers and concentration of the precursor salts must be known. Even small changes in stoichiometry[190,191] or residual of the chemicals synthesis[192] can have severe effects on the perovskite morphology formation and thus device performance as well as stability. Additional impacts are caused by the choice of solvents,[45,54,193] additives[194–196] lead salts[197] and their residuals[198–200] as well as the cations.[48,197] We note that the importance of small residual additives as passivation agents[62,194] and for engineering of wetting and crystallization has increased in recent years.[201,202] This is why precise description and control of solution composition down to very small molar contributions has become even more crucial for reproducing experiments. We highly recommend using the detailed table for specifying solutions in publications instead of plain text, as for example provided by Goetz et al.[76]

Solution Handling During Preparation: For specifying the perovskite solution completely, not only the exact composition but also the handling of the solution comes into play. When the solution is prepared, extensive stirring[203] as well as elevated temperatures[204] or filtering might be used, which can impact nucleation, later on. The reason is that perovskite solutions are known for the formation of iodoplumbate complexes[205] and colloids.[206,207] When handling the solution in a different manner or in a different atmosphere (see parameter above), the microstructure of the solution may differ, inducing changes in the subsequent crystallization dynamics.

Solution Resting Time and Handling after Preparation: After the preparation of the perovskite solution, it is important how long the solution rests before the coating process is started. This is due to the fact that many perovskite solutions are unstable and degrade as they age.[208–210] Possible reasons are the interaction with the surrounding atmosphere through hydration[211–213] or decomposition of solute components such as methylammonium iodide.[214] On the contrary, there are instances of beneficial effects of aging that help with the formation performant perovskite absorber film.[215] In addition, if the solution is stirred continuously after preparation or filtered/shaken again before deposition, this information should be provided.

Substrate Type/Materials: The substrate material must be reported as its properties can impact the fabrication of the perovskite film, later on. We define the substrate as the part of the PSC that does not participate in the electronic functionality of the PSC.[216] Key properties of substrates are their elasticity and rigidity as measured by Youngs modulus, their heat capacity, -conduction and -expansion, temperature stability as well as their thickness, roughness, and tolerance. All of these factors can have an impact on the subsequent fabrication steps. Most prominently, it is challenging to fabricate a PSC on flexible substrates due to a harder control of wetting and perovskite formation on these substrates, possible stresses on the perovskite, the functional layers, and the interfaces during bending and stretching.[217–219] It is good practice to not only report the substrate material (glass, metal foils, Polyethylene terephthalate, polyethylene naphthalate, etc.) and thickness but also the supplier and, if available, surface profilometry measurements or similar characterization methods on pristine substrates. We further note that substrate properties play a major role in annealing processes described later because these dictate how fast the temperature of the thin film changes upon heating and cooling. The substrate material can further induce thermal stresses due to thermal expansion.

Substrate Handling, Preparation and Substrate Holder: Substrate preparation, for example by cleaning, is a critical step in the fabrication of PSCs, directly impacting film quality, device performance, and reproducibility.[220] Any residual contaminants—such as dust, organics, or metal particles—can influence the nucleation and crystallization of the perovskite layer, potentially leading to defects, pinholes, or poor film adhesion. These imperfections reduce charge carrier mobility and increase recombina-

tion losses, ultimately lowering the device efficiency and stability. A substrate cleaned in a well-specified manner ensures a uniform surface energy, promoting homogeneous film formation and enabling consistent manufacturing outcomes. This is essential for laboratory research and scalable production.

Further, not only the substrate itself, but also the holder of the substrate can be crucial for the resulting perovskite film. For rigid substrates, the substrate holder's topology, leveling, and precision with possibly included vacuum suction points can have an impact on the shape and bending of the substrate surface. In a similar way, the tension and leveling of floating flexible substrates as well as the adhesion method of fixed flexible substrates, are decisive for their surface curvature. These particularities are only very rarely mentioned in literature. A photograph and technical drawing with tolerances of the used holder can make a great difference in the attempt to reproduce results.[221]

Substrate Dimension and Area of Interest: For being able to reproduce a solution deposition process, the extent and exact position of the area of interest[222] on the substrate play a major role. Most coating methods are inhomogeneous on the lateral scale.[4] For fully scalable coating methods such as slot-die coating, screen printing, and spray coating, these issues decrease (in the ideal case) with the substrate size. Non-scalable methods like spin coating or blade coating exhibit inverse behavior. Notably, for all common drying/quenching methods, the involved mass transfer dynamics are inhomogeneous on the lateral scale,[117] as well. For example, mass transfer peaks sharply under a gas nozzle (or "air knife") and falls off to the edges in a smooth way. Therefore, quenching might be less effective toward the edges of the substrate, but mass transfer is more homogeneous in this region.[117] In the same way, in case a linear air flow is used, mass transfer is highest at the edge of the substrate and falls off along the direction of air flow as the air saturates with solvent.[143] Also for natural drying, inhomogeneities can arise due to the shape of convection cells in the gas phase[223] and the higher surface-to-volume ratio at the edges of the film. It is therefore crucial to report which extract of the substrate area a particular analysis is focused on.

Substrate Movement: Substrate movement during processing must be taken into account because it dynamically impacts the mass transfer conditions. By moving a sample linearly under a jet of gas, for example, mass transfer is effectively integrated by subjecting the film to many different conditions in a timely succession. A similar observation holds for the rotational movement induced by spin coating.[224,225] Since perovskite crystallization occurs at a certain point in time, it might also be helpful to adjust the movement of the substrate. In this way, the nucleation occurs at a certain position (or moment) during the movement (for example the position of maximum mass transfer).[117] Additionally, substrate movement can continuously reshape the solution thin film as is the case in spin coating.[226] Further, movement relative to the quenching medium might have an effect. This is the case, for instance, when a flexible substrate is moved through a bath of antisolvent. Another example is the spinning of the substrate in antisolvent (or air) establishing a radial flow over the substrate.[226–229] If the velocity of the quenching jet is much higher than the movement speed, this effect can be neglected.

Substrate (or Perovskite Film) Temperature: Substrate temperature is one of the most important parameters when depositing perovskite solution films. Typically, it is assumed that heat conduction between the substrate and the very thin, deposited solution film is sufficiently high such that the solution film immediately stabilizes at the same temperature. However, the substrate itself has a certain heat capacity and conduction, which governs how its temperature changes over time. The film temperature, in turn, severely impacts both the crystallization and drying dynamics.[133,205,230] In case the atmosphere (or quenching medium) temperature differs greatly from the substrate temperature, heat transfer from the environment can no longer be neglected. For example, when using a hot air gun[231] or a preheated antisolvent,[232] temperature of the quenching medium must be reported. Under these circumstances, it becomes possible that, upon contact with the externally heated medium, the perovskite thin film gradually heats up (or cools down).[233] When drying a perovskite thin film fast, evaporative cooling may also come into play and must be accounted for in the energy and mass balance.[233] This becomes especially challenging when free-floating flexible substrates are used that have limited thermal contact to the exterior. It is preferable for reproducing results to constrain process parameters to extreme cases where heat conduction reaches an equilibrium such that the film temperature equals the substrate temperature. This reduces the complexity of the setup and facilitates reproducibility and modeling of process dynamics.[133] If this cannot be implemented, it is good practice to measure the temperature evolution over time with an infrared camera or a thermocouple.

Previously Deposited Layers/Substrate Surface: The previously deposited layer and its surface energy have an influence on the perovskite solution deposition and crystallization. For one thing, the preceding layer impacts the rheological properties, such as wetting measured commonly by the contact angle. The contact angle (or surface energy) directly governs the deposited wet film thickness when coating the perovskite solution (see next parameter). This is especially crucial for droplet-based deposition, such as used in inkjet printing[234,235] or spray coating.[236] For another thing, the pre-deposited layer can directly influence perovskite nucleation and crystal growth by offering nucleation sites and/or preferred growth directions.[237–239]

Contact Angle or Wettability: As mentioned before, wettability (or surface energy) as measured by the contact angle is a critical parameter. It depends not only on the substrate itself but also on the used solution (parameter introduced earlier). It is typically quantified with contact angle measurements that are facile enough to be executed for every perovskite solution process. In this way, differences between laboratory settings can be detected more easily. Wetting not only influences the coating process but also crystallization and film formation during perovskite deposition.[240,241] Processes affecting wettability, such as washing (see again parameter 'substrate handling') and/or plasma etching (also known as 'UV ozone treatment') should be properly specified with duration and intensity. Washing impacts the wetting and the adhesion to the subsequent layers and can potentially damage the preceding layers. In addition, the time after plasma treatment and washing is a critical parameter because those surface treatments are sometimes reversible with time in ambient conditions.[242,243]

Deposited Wet Film Thickness or Coating Parameters: The thickness of the initial wet perovskite solution film before the

drying or quenching process determines the outcome of the perovskite solution deposition process. Depending on the used coating technique, a variety of parameters such as the surface energy of the precedent layer, the surface tension, density, and viscosity of the solution, the solution sheering speed, and the vapor pressure (some of the solvent evaporates already during coating before any quenching), can impact the resulting deposited wet film thickness.[244–246] It might be challenging to define the wet film thickness because evaporation can start immediately after the coating process. In this case, only the coating parameters can be reported.[247,248] In particular, for batch-to-batch coating and droplet-based coating techniques, the film surface may be inhomogeneous. This can lead to the edges of the film drying faster than the center and Marangoni convection cells inside the film, fueled by the internal concentration gradients.[249–251] In some instances, measuring the volatile wet film thickness after coating is challenging.[109,133] This is why the specification of this parameter cannot be expected to be directly measured in all reports. However, as an easy alternative, it can be an option to measure the thickness of the crystallized film and then estimate the initial wet film thickness by producing this film thickness from material densities.[117] Alternatively, a full specification of the involved fluid and coating parameters (viscosity, surface energies, densities, additional rheological parameters, coating speeds, droplet size and ejection rates, ...) is equivalent to the parameter of the wet film thickness and enforces reproducibility. The great advantage of determining wet film thicknesses is that it allows for a comparison of processing conditions across different coating techniques.

Time to Quenching Onset/Time to Second Step Application: A notable parameter dictating the effectiveness or outcome of quenching is the time the wet film had to dry before quenching was performed. The same is true for the application of the second step in two-step deposition where residuals of solvent can impact the diffusion of the cations into the lead halide layer.[155] This is often referred to as waiting time or delay time. Due to the high boiling point of the employed polar solvents, perovskite and lead halide solution films exhibit a very slow drying rate at room temperature. The drying rate can be further reduced when intermediate phases are involved.[117] If the employed quenching method or the second step deposition are resilient to variations in the initial film thickness, the time to the next step might be less relevant. This case is occasionally referred to as the presence of a wide processing window.[252,253] However, especially when low-boiling point solvents, elevated temperatures and/or an unstable precursor solutions are used, the time until the second step is started can become a very important parameter. Accordingly, the time before quenching has been identified as a critical parameter by Zhang et al.[90] and Hamill et al.[254] and it is optimized in many other reports. Afterall, we are convinced that the parameter should be reported (which is mostly the case when using antisolvent quenching as we will see in section 4).

3.2. One-Step Processing

3.2.1. Impinging Jet Quenching Using Antisolvent or Gas

In the scenario of an impinging jet of a quenching medium flowing over the substrate (see **Figure 2**a,b), the mass transfer (as given by the Sherwood number) is well-defined exactly when the parameters given below are specified.[147]

Medium Ejected from the Nozzle: The type of medium used for quenching plays an important role for defining process control in quenching. Especially for gas quenching and vacuum (-assisted) quenching methods, it is not straightforward to identify the medium flowing over the perovskite thin film. For example, if nitrogen is ejected from a nozzle in ambient air, the ejected air stream quickly mixes with the ambient air through turbulence and diffusion.[257] Thereby, the quenching medium impacting the perovskite thin film is not well-defined. For the magnitude of the mass transfer, this plays only a minor role since the properties of different gases are very close to those of the ideal gas. However, the composition of the drying gas can still impact the perovskite morphology formation through indirect effects, such as the diffusion of water or oxygen into the thin film or catalytic impacts of these species on the morphology formation.[258] Furthermore, both in vacuum(-assisted) quenching and in glovebox systems, it is possible that solvent vapor builds up in the confined volume if the air is not extracted or filtered fast enough. To establish reproducible conditions, there are several options: 1) Use the same medium for quenching as is present around the substrate, 2) ensure proper circulation and flow conditions, 3) limit the solvent use in a glovebox to avoid buildup of solvent vapor. For antisolvent quenching, the film is covered by the antisolvent during quenching. This method might therefore be more resilient to different atmospheres. A saturation of the atmosphere with the gaseous antisolvent or other variations of the atmosphere can, however, still impact the crystallization dynamics before or after the quenching, as alluded to before.

Nozzle(s) Geometry and Size: Typical nozzle geometries are round and slot nozzles, for which mass transfer correlations are well-defined[259,260] (see Figure 2c). However, also nozzle fields and combinations of suction and ejection nozzles can be used.[161,255,261] In this case, nozzle width (and potentially nozzle spacing) must be fully provided (the best practice is to provide mass/heat transport coefficients directly[117,131] instead). Otherwise, mass transfer at the interface between the film and the flow medium is not well defined, making a reproduction of the results challenging unless authors provide a full Computer Aided Design (CAD) drawing of their setup. For antisolvent quenching, standardization of pipette tips in certain volume ranges can help to reproduce experiments.[262] However, this is very inaccurate due to the possibility to choose different pipette sizes for the same amounts of used antisolvent or differences in pipette design across suppliers (even intentional manipulation of the pipette openings are commonly employed). This is why explicit reporting of the tip diameter cannot be substituted by specification of the antisolvent volume.[263] The size and geometry of the nozzle or nozzles impact the homogeneity of mass transfer dynamics directly and thus govern how effective and homogenous the quenching will be on the selected area of interest.[255] As mentioned above, substrate movement can become important to balance inhomogeneities in the mass transfer induced by the nozzle geometry.

Nozzle Distance from the Sample: The third important parameter is the distance of the nozzle from the thin film (for mass transfer calculations it is usually defined as the distance of a line along the direction of air flow until it hits the sample).[264] In

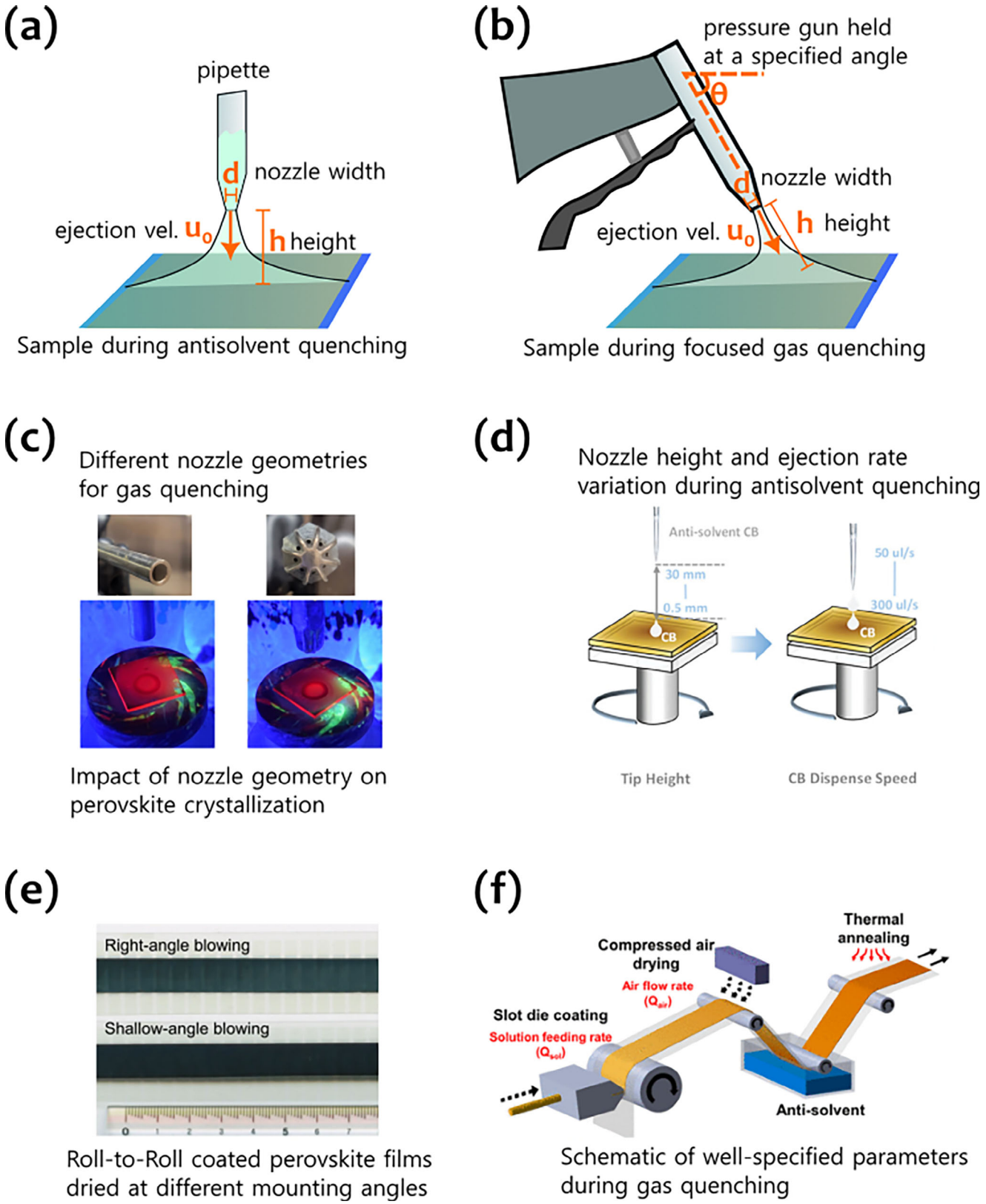

Figure 2. a) Impinging jet quenching using antisolvent ejected from a pipette with involved parameters ejection velocity u_0, nozzle width d, height h, (orange) and b) using high-pressure gas ejected from an air gun with involved parameters velocity u_0, nozzle width d, height h and impingement angle θ (orange). It is also possible to use an air knife with a slot nozzle or nozzle field (not shown here). The similarity between (a) and (b) methods becomes evident in view of the illustration. c) Two different nozzle geometries employed in gas quenching. Reproduced from ref. [255] (supplementary) with

the work of Zhang et al., the control of this parameter proves essential for optimizing the perovskite device performance[90] (see Figure 2d). It is therefore very likely that operators already optimize the parameter unconsciously in the laboratory. Distance is crucial for striking a tradeoff between homogeneity and magnitude of mass transfer.[117] When choosing distances closer to the sample, the mass transfer peaks under the nozzle center. However the difference between this peak and the outer edges of the substrate is more pronounced. In turn, the magnitude of mass transfer governs the formation of the perovskite morphology.[117] In some cases, the direction of movement can play an important role in balancing the remaining inhomogeneities. For spin coating, the rapid rotation enforces homogenization of areas in a radial dependence around the center of rotation (see homogeneity of the PL response as measured by Zhang et al.).[90] Interestingly, nozzle distance is often directly specified in gas quenching. However, in publications of antisolvent quenching it is mostly not defined (details follow in Section 4).

Nozzle Output Velocity (Alt. Pressure, or Air Gun Model and Setting): An important parameter dictating the flow of the quenching medium over the substrate – and thus the apparent mass transfer – is the flow velocity of the medium at the nozzle opening. Practically, for antisolvent quenching, this parameter is equivalent to the ejection rate of solution volume per unit time when the nozzle geometry is correctly specified. Empirical evidence suggests that the flow velocity is a crucial parameter for some classes of antisolvents, while it might be less important for another class of antisolvents[265] (this is related to solubility differences and the high effectiveness of the methodology making it resilient to parameter variation).[104] Nevertheless, an estimation of flow velocity is crucial for specifying the process correctly such that it can be transferred to large-scale deposition and/or reproduced in other laboratories. For gas quenching, air velocity is a very important parameter because gas quenching is less effective than antisolvent quenching.[104] Hou et al. find that air flow has a tangible impact on the perovskite morphology and thus the device performance[225] (this can be partially reduced when using a more resilient solvent system). In most cases, higher air flow velocities are favorable for quenching because they enable a quicker increase in supersaturation of the solution, which governs the effectiveness of quenching. However, when applying too high airflows, the film surface can become unstable and mass transfer becomes more inhomogeneous.[117,131] Interestingly, in many reports based on gas quenching, the static gas pressure at some point of the pressured air line before the nozzle instead of the air flow rate is reported.[47,225,266] However, static pressure at a certain position is highly dependent on the used air flow pipes leading to and away from the measurement position as well as the nozzle geometry.[225] Accordingly, Hu et al. report that the static pressure changes when the gas nozzle is opened and reaches a working pressure value.[225] Still, the pressurizing system and piping typically vary from one laboratory to another.[267] So, equal static and working pressure values in two different laboratories do not necessarily correspond to an equal rate of air flow through the nozzle. Therefore, it is good practice to measure air flow rate in standard liters per minute by a mass flow controller.[117]

Impingement Angle of Jet Onto the Solution Film: The impingement angle can have a direct effect on the homogeneity of mass transfer and the quenching effectiveness. For antisolvent quenching, mostly angles equal (or close to) 90° are used such that the jet impinges perpendicularly. However, when linearly moving the substrate, the jet angle is very often tilted. In this way, undesired pre-drying of the solution prior to the crystallization onset is suppressed,[131] enabling rapid drying under the nozzle center while avoiding an early crystallization (see Figure 2e). When varying the angle, it must be considered that shallow angles may decrease maximum mass transfer in the center region. Further, they can detrimentally impact the lateral inhomogeneity of the induced mass transfer.[117] Mass transfer correlations for tilted angles show that it is not possible to avoid any airflow in an undesired direction completely when using high output gas velocities (unless by transitioning to a linear air flow configuration).[117,264]

3.2.2. Linear Flow Quenching

Linear flow geometries have become more popular recently due to the advent of vacuum-assisted quenching.[133] In the highly reproducible setup of (approximately) 1D flow over the substrate (see **Figure 3**a,b), the air is extracted from one side of a closed chamber and/or pushed into another side of the chamber (in fact, complex flows in more dimensions can arise which make reproduction of results challenging).[268] Depending on the magnitudes of influx and outflux, a pressure decay can be achieved.[104,141] The solution film is then dried by the induced air stream that can be laminar or turbulent depending on its Reynolds number.[147] According to Sherwood correlations for laminar (turbulent) air flows, the following parameters must be specified:[147]

Flow Geometry: In the case of a linear air flow, the geometry of the whole chamber used for quenching dictates the drying dynamics.[104,268] Further, the part of the sample where the air flow impinges will experience the fastest drying.[143,269] Along the direction of air flow, the evaporation rate decreases because already solvent-saturated air will dry the sample less effectively (see Figure 3c). It is also possible that the shape of the substrate itself impacts the air stream and the mass transfer. Therefore, it is advisable to provide CAD drawings of flow chambers to aid in reproducing the results. In vacuum(-assisted) quenching, one needs

permission of the authors, 2023. d) The parameters tip height (30 to 0.5 mm) and dispense speed/volume rate (50–300mul s^{-1}) that were shown to be impactful in automatized antisolvent quenching. Reproduced from ref. [90] with permission from John Wiley and Sons, 2023. e) Showing the advantage of shallow angle blowing when using a slot nozzle and high-pressure gas. By blowing at a shallow angle, the solution film is less influenced by the drying air before the onset of quenching, where mass transport is exceptionally high. Reproduced from ref. [256] with permission from, Springer Nature Limited 2023. f) An exemplary, fully defined jet-based quenching process (that is followed by an additional antisolvent process) as described in the work of Ham[144] et al. In their report, they describe the use of compressed air with varying flow rates from 5 to 30 L min^{-1}. They further report that the air nozzle was installed at a distance of ≈60 cm, that the gap between the nozzle and the film was 5 cm, and that the dimensions of the air nozzle were 10 cm wide and 200µm thick. Reproduced with permission from ref. [144] Copyright 2021 American Chemical Society.

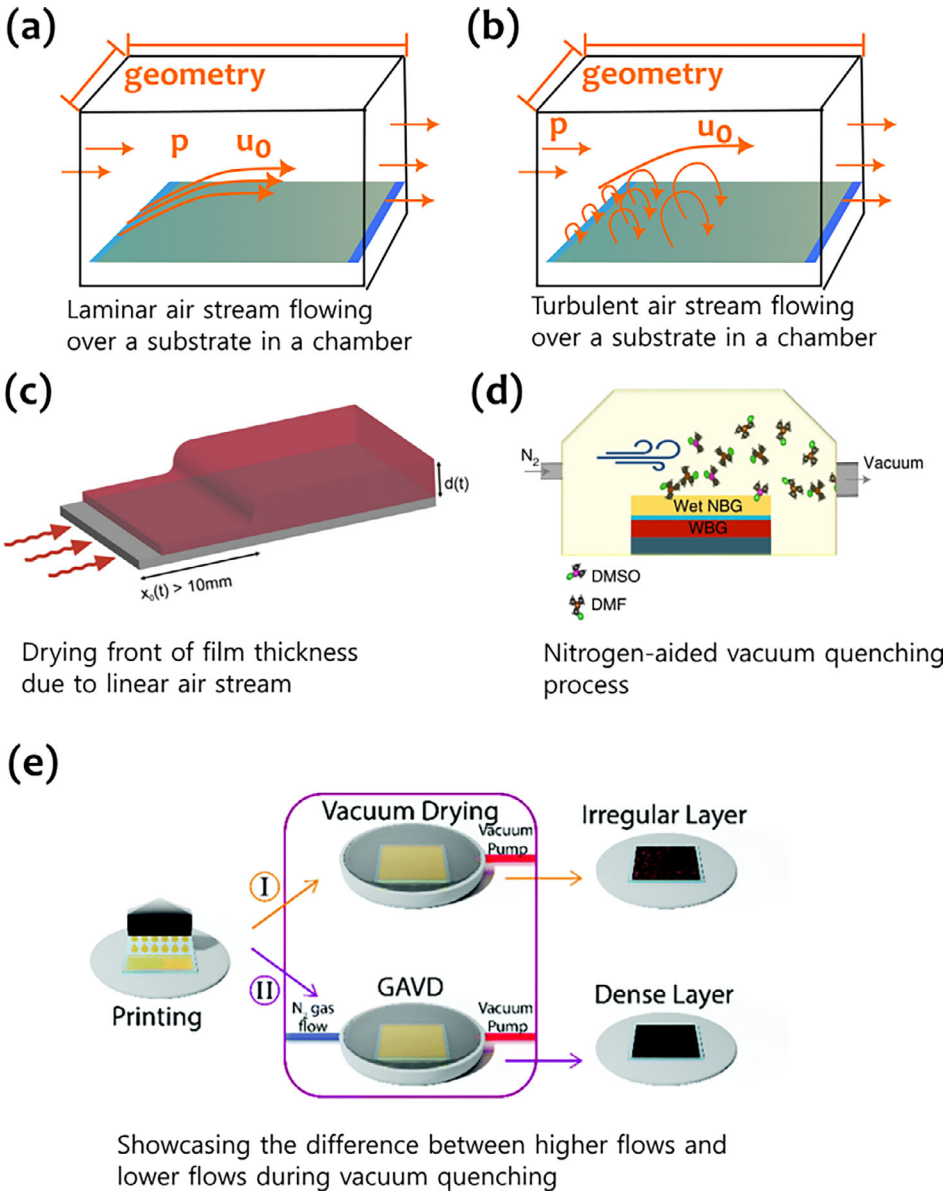

Figure 3. Linear flow quenching with a) laminar and b) turbulent air flow. The most important parameters are the pressure, p, the air flow velocity u_0 and the geometry of the flow channel The magnitude of the Reynolds number determines the likelihood of the formation of turbulences.[147] c) Schematic of a drying front as produced by a linearly impinging air flow.[143] Reproduced from ref. [143], with permission from Elsevier. d) Depiction of vacuum-assisted quenching by Abdollahi et al. They specify the time, the pressure decay as well as the input flow of N_2 during vacuum quenching, noting for each point in time the crystallization onset. Reproduced from ref. [141] with permission from the Springer Nature, 2022. e) Demonstration of gas-flow-assisted vacuum drying (GAVD). In the first case, the air is simply extracted at one side of the chamber, while in the second case, an additional N2 supply increases the (undefined) gas velocity. Reproduced with permission from ref. [139] The Royal Society of Chemistry, 2021.

to take into account the additional complex interplay between the pump power and extraction rate, the pre-pumped pipe volume connected to the chamber, the chamber volume, the chamber width and height in relation to the substrate size.[104] All of these aspects impact the (time-dependent) flow velocity, as well as the time-dependent pressure decay inside of a vacuum chamber when the nozzle is opened. Therefore, to reproduce vacuum-assisted quenching, the pump model, the pipes leading to the chamber, as well as the chamber geometry should be exactly specified.

Flow Velocity: Just as in the case of impinging jet quenching, the flow velocity at a certain distance over the sample (that is outside the hydrodynamic boundary layer) should be measured and specified. For a linear air flow at atmospheric pressure, the flow velocity can be measured by a hot wire anemometer, a pitot tube, or, alternatively, by a mass flow controller at the input and/or output. For vacuum(-assisted) quenching, the flow velocity depends on a complex interplay of multiple factors: The strength of the pump, characteristics of the valve opened to start the process, the piping leading to the pump introducing potential dead

volume already at low pressure and intentional or unintentional leaks. In a vacuum chamber, it can be challenging to measure the flow velocity directly, so the mass flow controller should be the more practical option[141] – enforcing reproducible conditions if the chamber geometry is correctly specified. Alternatively, the drying dynamics of a reference material system can be measured directly with optical in situ characterization, allowing for an indirect determination of the apparent air flow.[104] The impact of air flow velocity during vacuum quenching is confirmed in multiple instances[104, 139–141] and is showcased in Figure 3d,e.

3.2.3. Natural Drying and/or Convective/Diffusive Quenching

Natural drying arising from convection and diffusion is present in a variety of different forms in laboratories and factories (see **Figure** 4a). The case where a film is immersed in a solvent resembles this case (see Figure 4b).

For Natural Drying: Geometry and Ventilation of Laboratory or Glovebox System: Reproducing conditions of natural drying is challenging because, in practice, there is rarely an undisturbed environment for natural convection. The latter can be influenced by a multitude of factors, having different impacts according to the frequency of the distortion.[146] Thus, well-defined natural convection could only form in a sufficiently large, leveled box of undisturbed gas that is isolated against vibrations from the exterior. However, in closed glovebox systems, there are usually moving parts (most importantly the gloves of the operator) inducing vibrations and air movements over the sample, thus disturbing natural convection. Likewise, when operating in a fume hood, there is a net laminar flow (and potential turbulence) due to air extraction. Conclusively, the setup corresponds rather to a linear flow as described above instead of natural drying. Additionally, laboratory safety standards enforce hard limits on air exchange rates, producing net air flow within the whole laboratory. Consequently, it is very hard (if not impossible) to specify natural convection in the laboratory in a way that is highly reproducible. If natural drying processes are reproducible, it is most likely the consequence of the choice of solution system such that similar morphology is achieved in varying drying conditions[148] (see Figure 4c) However, even in this case, well-defined drying conditions help to enforce a better consistency of the presented results. To improve reproducibility, the air flow due to ventilation in the room can be monitored or the response of the process to intentionally altered drying conditions (e.g. by placing ventilators) should be tested and/or reported.

For Antisolvent Bath: Vessel and Method of Immersing the Substrate: For antisolvent quenching by immersion of the substrate, a similar problematic arises as is the case for the gas quenching with natural drying. To implement natural convection and/or diffusion based antisolvent quenching, the substrate must be immersed with the antisolvent or moved into the antisolvent bath. Both procedures however induce a considerable fluent flow within the bath or container the antisolvent is kept in. In the case where the substrate is moved linearly through the antisolvent,[144] the net flow might even resemble laminar flow. In some reports, intentional (turbulent) flow is induced by stirring the antisolvent,[270] which most likely improves the reproducibility (see Figure 4d). We conclude by stating that, whenever using antisolvent bathes and/or natural drying, videos of the experiment might be especially helpful for reproducing the result.

3.2.4. Radiation/Thermal Quenching in One-Step Deposition

In addition to the above quenching methods, which cover almost the entirety of one-step device fabrication, there are some quenching methods that are not described by mass transfer of solvents alone. These methods include significant heat transfer and/or other particle interactions such as the absorption of incident radiation. We distinguish radiation-based and thermal conduction-based methods[271] (see **Figure** 5a,b). Interestingly, to describe radiation or thermal-based quenching, an analogy to impinging jet-based quenching can be drawn. The parameters are given by the type of irradiation (media used for quenching), radiation source geometry (nozzle or radiator size and geometry), distance and angle from the sample and intensity of emitted radiation (flow velocity).

Kind of Radiation or Heat Source used for Quenching: The kind of radiation or heat source used for quenching is crucial for this methodology. The most common heat source is a hotplate onto which the sample is placed. For this kind of heat source, it must be considered that the substrate surface (as well as the substrate back surface) can be uneven. This introduces an inhomogeneous air gap between the substrate and the heat source. So, for achieving homogeneous heat conduction and consequently a homogeneous heat distribution over the substrate, it is of merit to control the gap between the heater and the substrate (which is also important for the annealing processes later on). The most common radiation type involves photons in the infrared spectrum[273] (see Figure 5c,d). This irradiation has, in essence, a very similar effect to the heat-induced method, since these photons are absorbed quickly over a wide range of materials.[122] So, infrared radiation is equivalent to a very localized heating that will quickly dissipate by additional heat conduction into the substrate. Just as thermal quenching, it may therefore combine quenching and annealing in one single workflow step,[122,123] which has potential advantages for cost-effective manufacturing. In addition, IR-annealing can be tweaked to a certain wavelength range corresponding to the excitation energy of the used solvents. Another example of radiation-induced quenching is plasma – involving incident charged ions, electrons and photon irradiation (see Figure 5e).[151,272] The radicalized ions, UV photons, and free electrons strongly interact with the film surface, inducing heat, but also directly vaporize, oxidize and/or radicalize the film surface. In this way, plasma can be a catalyst for chemical reactions (and in particular crystallization).[272]

Radiation Source Geometry/Heat Source Geometry: The geometry of the used heat source cannot be neglected because it heavily impacts the homogeneity of the temperature distribution. First of all, the placement of the heat or radiation source relative to the substrates must be specified because it can influence the direction of crystal growth.[274] Typically, hotplates are placed under the substrate, while infrared annealing is carried our from the top downward. When using hotplates, it must be considered that these often do not operate with homogeneous temperature distribution, which becomes more pronounced the higher the temperature increases. Therefore, it is good practice to specify

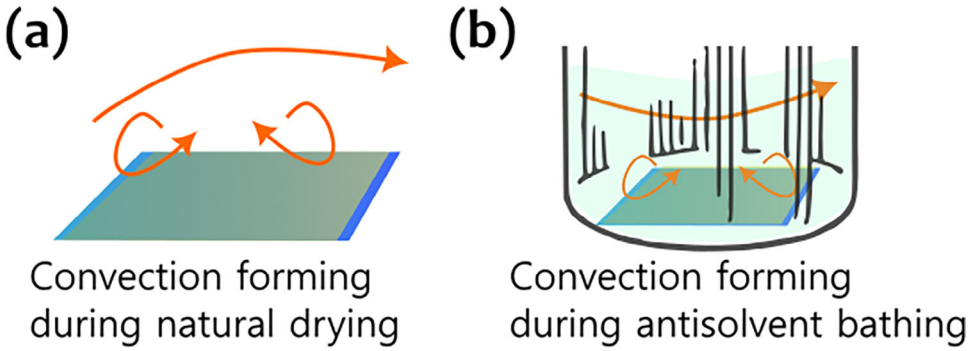

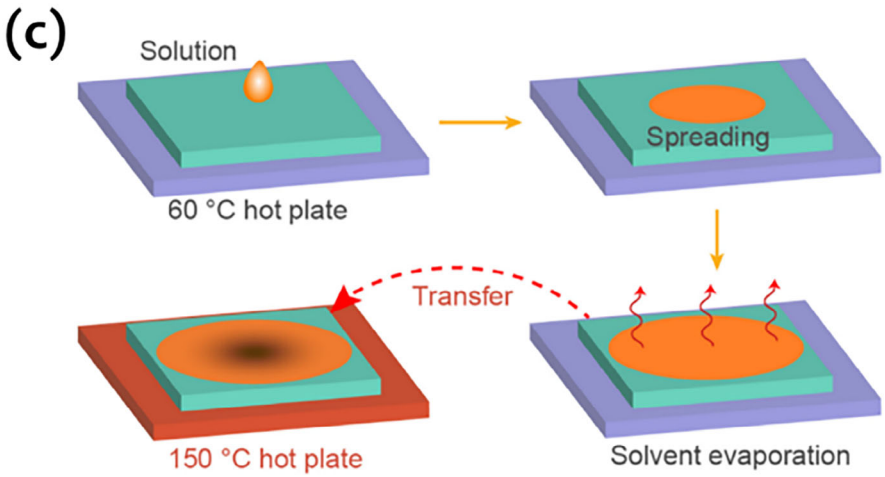

Schematic of fabricating high-quality perovskite films by drop casting and natural drying

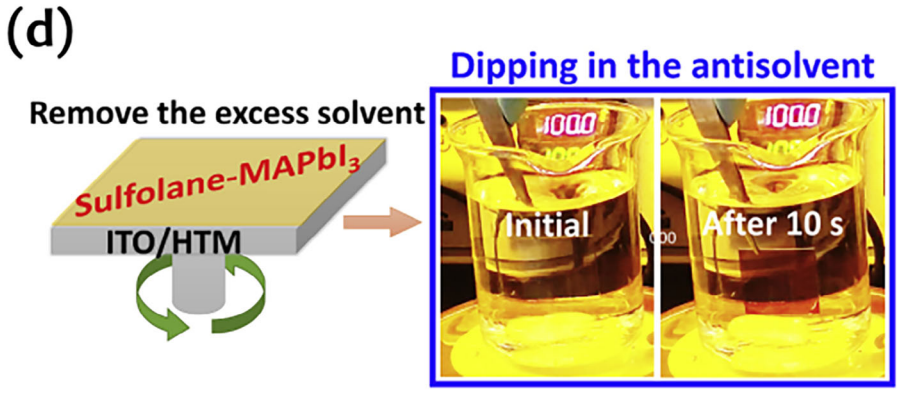

High-quality perovskite films fabricated in a stirred antisolvent bath captured before and after quenching

Figure 4. Natural drying a) and immersion of a substrate in an antisolvent b) resembling the situation in (a). There are no well-defined parameters indicated because natural convection and diffusion can be influenced by many factors. In the ideal case, there are no parameters required except the temperature of the medium (already specified in the general parameters) and the properties of the medium and the materials in the film. However, in a real laboratory or factory setting, it is very likely that the surrounding medium is moving due the movement of the substrate or exterior influences as indicated by the orange arrows. c) Perovskite films fabricated with natural drying by an optimized perovskite composition as demonstrated by Zuo et al.

the hotplate manufacturer as well as the dimension and, in the ideal case, capture the thermal distribution with a thermal camera (see Figure 5d). In a similar way, each radiation source has a specific directional profile of emission of radiation defined by its geometry. For example, infrared light typically consists of a bar-type symmetry including infrared mirrors. These are decisive for the radiation intensity and direction impacting the thin film. For plasma sources, the nozzle form and orientation of the discharge chamber come into play as important parameters that would need to be considered for describing it consistently (see again Figure 5e).[151]

Outgoing Intensity of Irradiation/Heat Flux: The heat flux onto the sample in contact with the hotplate is decisive for the morphological transformation. It can be estimated from the substrate's and hotplate's heat conductive properties and temperatures or, alternatively, measured by recording the temperature change over time and fitting the corresponding differential equations.[233] When using radiation, the intensity, i.e. the mean energy per unit area and time, is a very important parameter. Typically, the incident intensity is not measured or known, but rather specified indirectly by the distance over the sample (see below). Only the intensity emitted by the used machine is specified (it is very important not to confuse the emitted IR intensity with the electrical power of the heating elements). Due to these considerations, a direct measurement of substrate temperature over time via infrared cameras or temperature sensors is advisable.

Distance of Radiation Source from the Sample/Distance of Heat Source from Sample: The distance of the radiation source from the sample is a very important parameter as the (divergent) radiation intensity typically decays with increasing distance. At the same time, the irradiated intensity might be more homogeneous at larger distances. In addition, the drying dynamics can be impacted by the distance, since the solvent vapor can build up under the radiation source. Also for a hotplate, distance from the heated surface is an important parameter.

Irradiation/Heating Time: When radiation or heat is used, a crucial additional parameter is given by the radiation (or annealing) time. Radiation and/or heat can alter the perovskite film substantially even after the crystallization process is completed. The reason is that both irradiation and temperature provide energy to the particles inside the perovskite lattice, inducing morphological restructuring and/or phase transitions. These can be beneficial for the crystallinity and optoelectronic quality of the thin films. However, when irradiating the sample for too long, it is possible that degradation might become an issue for fabricating high-quality perovskite absorber films.[123,150]

3.3. Two-Step Processing

Herein, we analyze the parameters crucial for two-step processing, in additional to the general parameters introduced in Section 3.1 (see again Figure 1). We distinguish two-step processing further according to two different methodologies routes for applying the AX solution. The most common method is the application of the AX solution by (dynamic) coating (see **Figure 6a,b**). However, it is also possible to apply the AX solution by immersion (see Figure 6c). According to the intrinsic logic of states and workflow steps introduced in Figure 1, we can automatically deduce many process parameters from one-step deposition that are required for two-step deposition. Below, we outline some particularities that need to be considered in two-step processes.

3.3.1. Additional Parameters

Drying conditions of Lead Halide Layer: Equivalent to the jet-based quenching (or laminar and natural drying) steps described in Section 3.2, the drying parameters of the BX_2 layer can influence its film morphology.[108] (Alternatively, the lead halide layer can be evaporated in the hybrid approach as vapor[158–160] or deposited from a spray or aerosol).[275,276] The morphology of the BX_2 layer is just an intermediate step for the perovskite film fabrication. Similar to one-step processing, it has been shown that porosity and surface coverage can be influenced directly by the drying conditions.[155, 277–279] These are, in turn, crucial for the diffusion of the cations into the lead halide layer, later on. If drying via an impinging jet or vacuum extraction is employed, we use the same parameters described in Sections 3.2.1 and 3.2.2. It is of utmost importance to know the structural quality of the lead halide (BX_2) film before applying the second step (AX solution). The authors highly recommend to report on these intermediate phase using optical and x-ray-based analytic methods for better comparability.

Drying Time of the Lead Halide Layer: The longer the BX_2 film is dried, the fewer solvent residuals remain in the thin film.[278] For example, due to the formation of PbI_2-solvent complexes, solvent residuals can be intercalated[280] such that evaporation is suppressed. Some solvent residuals can be desirable because they facilitate diffusion of the cations into the layer later on.[281]

Annealing Parameters of Lead Halide (If Annealing is Performed): After the first deposition, some groups perform an annealing step of the BX_2 layer alone.[279, 282–284] This step can impact the morphology of the obtained BX_2 film as dictated by the temperature.[282] For details on the involved parameters, we refer to Section 3.4 where the annealing of the perovskite layer is explained. Again, just as for the perovskite annealing, the annealing time of the BX_2 can play an important role in the final device morphology. The longer the annealing is executed, the less solvent residuals will remain within the BX_2 film. The morphology formation of the BX_2 layer can also be influenced by the surrounding atmosphere and, in the same way, the hotplate geometry. Thus, in case annealing is used, we obtain four additional parameters for the annealing process of the BX_2 alone, just as we find later for the annealing of the perovskite film.

Reproduced with permission from ref. [148] by Elsevier, 2023. d) Photos and pictogram of the antisolvent immersion method described by Huang et al. In the supplementary, they provide a video of their method for making scalable perovskite thin films.[270] They stir the antisolvent continuously, which – in contrast to pure natural convection – induces a complex, forced flow of antisolvent over the thin film forming a boundary layer. So, strictly speaking, the conditions for reproducible natural/diffusive quenching are not met. Reproduced from ref. [270], Copyright 2021 with permission from Elsevier.

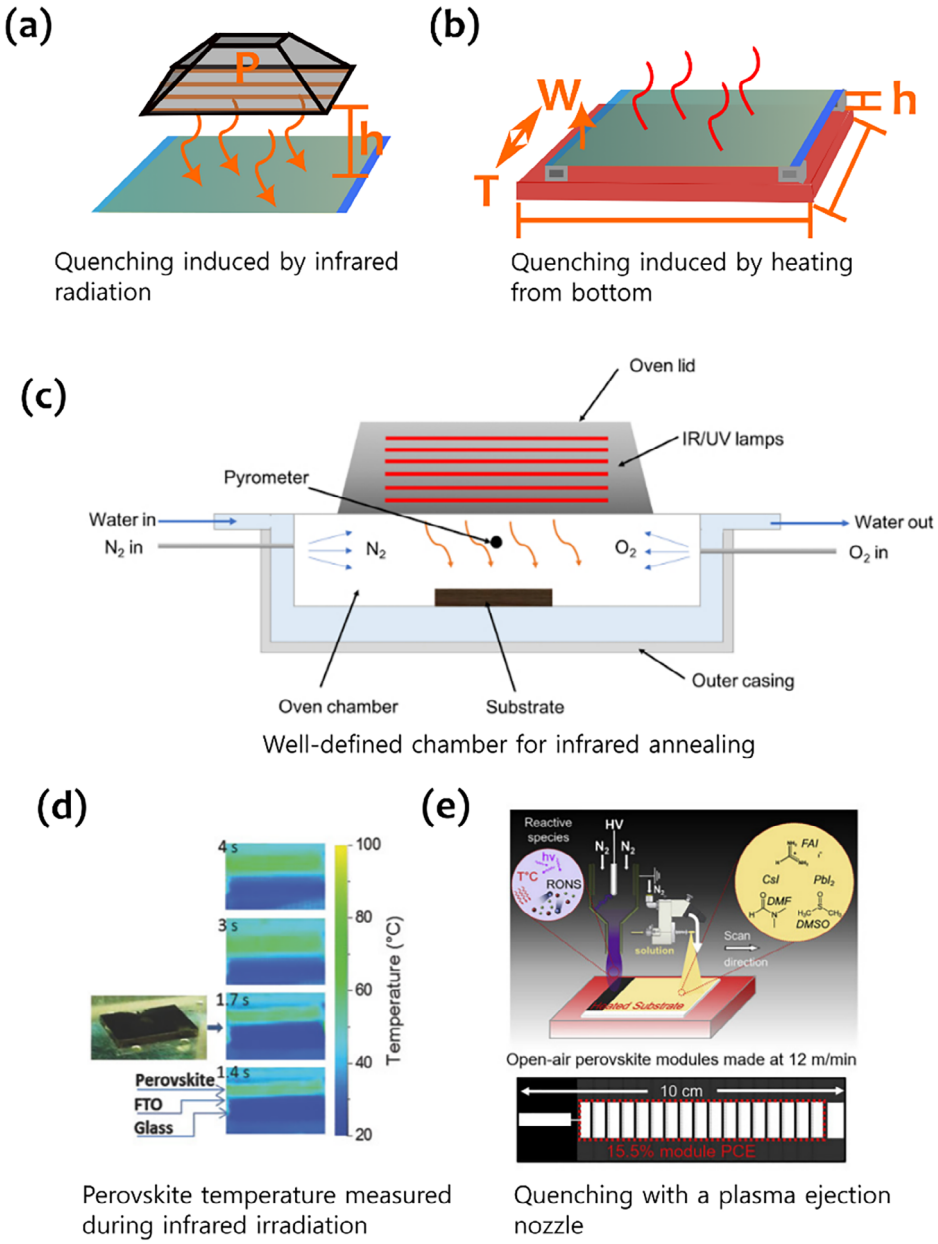

Figure 5. Infrared quenching a) with height over the substrate, d, the power, P, and the geometry of the radiator bars and thermal induced quenching b) with a geometry, a distance from the hotplate, d, the hotplate temperature, T, on a hotplate. c) the work of Ling et al. This is reproduced with permission from ref. [152] by JoVE and d) the works of Sanchez et al. Reproduced with permission from ref. [123] by Wiley and Sons, 2018. Both use well-defined infrared-induced quenching. While they do not specify all dimensions in the experimental setup, they still measure directly the temperature effects of the infrared radiation on the sample area.[123,152] In this way, reproducible conditions are enforced that can be leveraged/compared when trying to replicate their process. e) Rolston et al. demonstrate plasma-induced, rapid conversion of the perovskite absorber thin film. Reproduced from ref. [272], Copyright 2020 with permission from Elsevier.

Composition of Cation Solution: Evidently, when the second step is carried out, the composition of the AX solution plays a major role in describing the mass transfer of A-cations and X-anions into the BX_2 film. At the same time, the properties and volatility of the solvents employed of the second coating step have an impact. For example, via the composition of the cation solution, the PbI_2 to cation ratio can be optimized.[283] Therefore, the solution composition of the cation solution must be specified.

3.3.2. Coating of the Cation Solution

Coating and Drying Parameters: When the second step is carried out, the environment and coating parameters dictate how the AX layer will be deposited on top of the BX_2 thin film (see Figure 6a,b). Typically, a solvent that does not dissolve the BX_2 is used. This is why this step can be regarded as a separate coating process. The coating process dictates how much AX solution

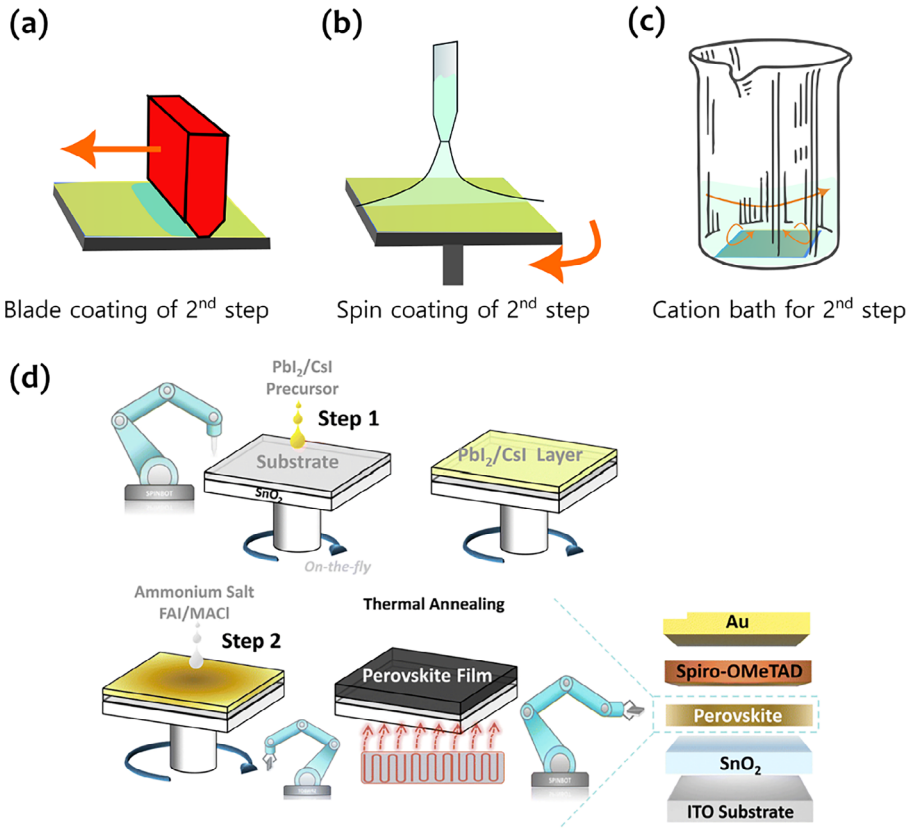

Figure 6. Two-step method with coating of the cation solution by a) blade coating and b) spin coating. c) Alternative method of immersion of the substrate for two-step processing. d) Fully automatized two-step deposition with control routines as introduced by Zhang et al. control the following process parameters of two-step processing with an automated device acceleration platform. Reproduced from ref. [82] with permission from Energy and Environmental Science, 2024. e) Atmosphere and gas flow speeds of step one and step two, spin durations, pipette tip height and solvent dripping speed. For every controlled parameter, they determine its impact on PCE and find that the dripping speed the second most impactful parameter directly after the spin speeds. Reproduced from ref. [81] with permission from John Wiley and Sons, 2025.

is available for reaction within the BX_2 scaffold. Just as in one-step processing, we define the coated wet film thickness as the most important parameter from coating (or alternatively a full disclosure of the coating and rheological material properties). It must be considered here that, unlike in one-step processes, the time of contact of the drop-cast AX solution prior to the start of the coating process can also be impactful.[285] This time should therefore be specified, or minimized by the use of dynamic coating. Another critical factor is how long the film remains in contact with the solvents and excess solutes of the AX solution after coating.[286] Further, the AX solution can be dried with enhanced air flow and/or elevated temperature and/or irradiation, just as in gas quenching of one-step perovskite.[122] In case these drying techniques are used, the corresponding parameters should be provided. So, according to the recurrent arrow in Figure 1 pointing upstream, we can introduce additional workflow steps in the application of the second step, for example using impinging jet drying, laminar air flow or natural drying (introducing 3,4,5 additional parameters respectively). We note that there is a particularity of dynamic spin coating, where the application of the second step can resemble the antisolvent quenching in one-step processing (see Figure 6c). Correspondingly, Zhang et al. showed that the rate of solution ejection from the pipette is decisive for the devices' PCEs[81] (see Figure 6d,e). In the schematic of Figure 1, it should therefore be discussed to treat the application of the second step under the category of quenching/drying and not as a coating step. A similar consideration applies for the bathing of a substrate in the cation solution. In this light, it is recommended to report the parameters for the chosen coating method as well as the corresponding quenching/drying process.

3.3.3. Immersion in Cation Solution

Vessel Geometry, Reaction Time, and Stirring/Immersion Method: When the second step is carried out by bathing the film in the AX solution, it becomes important how long the BX_2 film is immersed. With more immersion time, the A-cations and X-anions have more time to react with the present BX_2. Further, in analogy to the antisolvent by bathing method, the method of immersion/stirring can play a vital role in these kind of processes because a flow within the AX solution can accelerate mass transfer from the solution into the BX_2 film and vice versa. A good solution to make the flow field within the bath more reproducible is to use continuous stirring and capture a video of the whole process.[270]

3.4. Final Parameters

To complete the perovskite morphology formation, some parameters come into focus that are important once the coating, quenching and/or second step application is completed. We note that annealing does not always coincide with the crystallization of the perovskite. Rather, annealing should be seen as a finalization of prior perovskite formation from a possible mixture of solvent, intermediate phases, and crystallites involving Ostwald ripening, grain growth, nucleation,[81,90,287,288] where the chemical environment can play a crucial catalytic role.[64, 289–291] In case thermal quenching is used, some of the following parameters can be omitted because the annealing and quenching are combined in one single step.

Time to Onset of Annealing: The time between the last processing step and the onset of the annealing process is important. It can influence the composition, microstructure, and distribution of material of the thin film when the annealing process is initiated.[133,292,293] When a delay is introduced, nucleation and agglomeration can start prior to the onset of annealing, influencing the final obtained morphology.[238,294]

Annealing Time: Since all chemical transformations as well as mass transfer dynamics are time-dependent, the annealing time plays also a crucial role during morphology formation.[295–298] It is desirable to choose the annealing time in way that maximizes the presence of the desired perovskite phase as compared to degraded phases such as PbI_2[295,297] to minimize pre-mature material degradation as well as the formation of undesired phases.[299–301]

Annealing Temperature: Annealing temperature is one of the driving factors for opto-electronic quality of perovskite thin films.[118, 302–309] All material diffusion parameters, as well as crystallization dynamics are highly temperature-dependent because temperature determines the average energy that a species has at its disposal for undergoing phase changes and chemical reactions. Concluding, it can be decisive for the resulting crystal structure,[307,308] phase composition, and stoichiometry.[309] Furthermore, a higher temperature also promotes the evaporation of volatile species at the film surface which can have a tangible impact on the film morphology at the end of annealing. As stated above in the section on heat-induced quenching, the temperature distribution of the used hotplate should be measured. It is beneficial to define the gap between the substrate and the hotplate exactly.

Annealing Atmosphere Composition and Temperature: During annealing, an exchange of mass through the film surface with the surrounding atmosphere becomes possible.[310,311] This mass exchange can occur in two directions. For one thing, humidity as well as oxygen can diffuse through the film surface into the film. For another thing, the opposite of the above processes is possible with additional solvent or cation salt residuals as well as halides being able to leave the film surface. The higher the annealing temperature, the more pronounced will be the process of volatile components leaving the film as compared to the inverse process. It is however also possible that the presence of humidity acts catalytically, opening new routes of chemical reactions or crystallization pathways through intermediates[54] and thereby influencing the forming morphology.[54,312] Further, the higher the temperature difference between the ambient air and the hotplate, the more pronounced the convective air flow over the hotplate area will be. This can accelerate the mass transfer in both directions further.

4. Overview Survey on Reporting Frequency of Process Parameters in Literature Domains

As demonstrated above, the process parameters of perovskite solution deposition open a multidimensional space for process control and optimization. The parameters described in Table 1 are relevant and required because 1) they were proven to have an

impact on perovskite film quality (see last section) and 2) pilot studies have shown the great relevance of such data for reducing variance of device performances and optimizing the vast available parameters space.[81,83,90,93] To illustrate the frequency of reporting of process parameters in state-of-the-art research reports, we conducted a small overview survey (see Supplementary Note 2 for sources and Tables S3–S6, Supporting Information for detailed data). The survey focuses on three important domains of research: 1) high-PCE PSCs fabricated with the one-step process (55 reports) 2) high-PCE PSCs fabricated with the two-step process (32 reports) and 3) state-of-the-art large-area perovskite modules fabricated by a one-step process (57 reports). Tables S5 and S7 (Supporting Information) list the corresponding references investigated in the survey. The tagging follows the convention: "yes" if a parameter was specified within the device fabrication section, "triv." if trivially specified (that is to say to an educated reader it is clear what the parameter value was, for instance, during antisolvent quenching, the pipette is held in a 90° angle):, "ind." if indirectly specified (the parameter is not explicitly specified, but in defense of these reports, we cannot rule out the possibility of estimating/deducing the parameter by doing extensive research: for instance, deducing the nozzle size from the used pipette tip type or model of the used air gun), "inc." if incompletely specified (for example, if the atmosphere type is specified as ambient, but humidity is not reported) or "no" if not specified/mentioned. If a certain parameter was not required for the used processing or quenching method according to the evidence presented above, it is annotated as not defined "n.d.". **Figure 7** contains a summary of the results of the survey. For every parameter, we list the percentage of reports specifying it correctly. For this analysis, we count the number of reports that specified (and indirectly/trivially specified) the respective parameter and divide the result by the number of reports, in which the parameters must be specified (provided above evidence for the chosen processing method). We note that, according to literature analysis above, all of the listed process parameters affect the perovskite morphology. Hence, the missing percentage of reporting of a parameter correlates with the potential for improving process reproducibility by controlling this parameter in the future. This does not mean that the parameter is not implicitly controlled when it is not reported. However, if a parameter is reported frequently, it is very likely controlled by most of the groups. Further, as mentioned above, the reporting of a parameter facilitates the reproduction of results in a different laboratory.

Regarding the results for high-PCE devices fabricated with one-step (top plot in Figure 7), we find that the specification of parameters in the literature varies by a great amount. Some parameters are (with unique exceptions) almost always reported, while some other parameters are almost never reported. Overall, we find a "specification gap" of ≈36% considering the parameters listed herein. Starting from the solution composition which was reported in all of the investigated reports, a steady decrease in the likelihood of reporting occurs for the remaining parameters sorted toward the right of the figure (we sorted the process paramters by their occurence in reports). This hints at an implicit agreement between researchers that some parameters (starting from the solution composition up to the nozzle size parameter) must always be specified in reports on PSCs. The agreement weakens consecutively for the parameters on the right of the nozzle size parameter and finally reach occurrences below 1% of reports for the distance of the nozzle during quenching. The reason is, most-likely, a mimicry effect. New reports use the same set of descriptive parameters as in previous publications – out of which early and high-impact works get priority. So, if a certain parameter was provided in one of these landmark works, it was adapted in most of the community (also the opposite is true). Out of the general parameters, the solution handling and resting time, the substrate size and temperature, as well as the atmosphere composition and temperature, are the ones where most potential in specification exists. Interestingly, especially the parameters of mass transfer during the quenching process, that is nozzle distance and output velocity (or ejection rate), are highly underspecified. For antisolvent quenching, the only quenching-specific parameter that is frequently reported is the used antisolvent volume that gives limited information about mass transfer. So, it is a considerable possibility that the use of different pipette tips, the distance from the sample and the rate of ejection (velocity of antisolvent) account for a huge fraction of the issues with reproducing this very common fabrication process. This is underlined by the fact that automation of these processes reduces the variation in the device performance.[81,82] Therefore, in regard to the evidence summarized above, we highly recommend to extend and strengthen the already existing consensus (or standard) to the remaining parameters described herein in accordance with the updated TFSCO. Closing the gap of the control and reporting of parameters could lead to a considerable increase in reproducibility of processing routines across different laboratories.

When comparing the one-step processes of small-scale PSCs to those of one-step fabrication on large-area devices with similar quenching methods (see Figure 7 middle plot), we find that there is a similar trend between very frequently (that is implicitly standardized) process parameters and not frequently reported parameters. There are however slight differences. While about half of the parameters are provided in almost all cases, sensibly, the substrate size is stressed more in reports on large-area PSC fabrication (Substrate size is however not very often provided for small-scale PSCs). The specification gap of ≈38% is not significantly higher than in the one-step small-area PSCs. Additionally, the nozzle size and the time to annealing are less often reported. The reason is that large-area fabrication is carried out more often in close-to industrial conditions, where gas quenching outside the glovebox is used as opposed to antisolvent quenching in glovebox.[313] Further, the annealing process is not necessarily carried out instantly after coating. Regarding the results obtained for high-PCE two-step processing of small-area PSCs (see bottom plot in Figure 7), a similar gap in reporting can be found as for the one-step processed PSCs (again ≈34%). Interestingly, the annealing atmosphere of the second step is specified with a much higher likelihood than that of the first step. The reason is that the second step is often carried out under ambient atmosphere with measured humidity, while the atmosphere in which the first step was processed is underspecified. In addition, the time of sample transfer between the coating and the annealing of the second step is underspecified. This is most likely because it is started as soon as possible after the coating process. More precise language (or a video of the fabrication) could help to clarify remaining differences between processes. We further investigated the correlation between the publication date and the number of citations with the

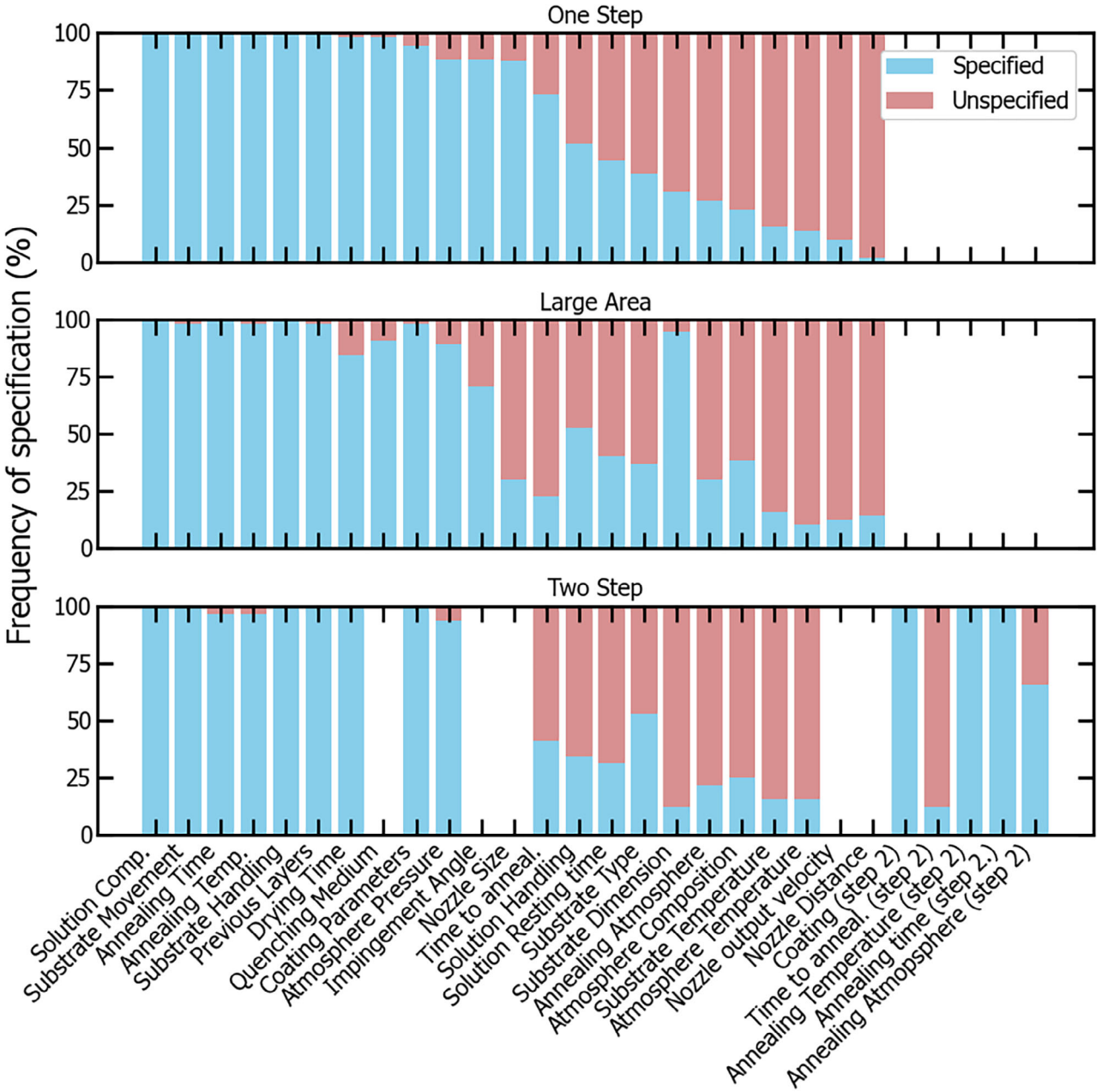

Figure 7. Percentage of reports specifying the respective parameter within the device fabrication section, supplementary or main text of (top) one-step devices (middle) large area devices with one-step fabrication and (bottom) two-step devices. The label "specified" means that a parameter is specified, indirectly specified or trivially specified. The label "unspecified" means the parameter is not specified or incompletely specified. (parameters who do not apply to a certain publication are not counted). Parameters are sorted according to occurrence in one-step processes. Parameters that do not apply to the respective method are left blank. The total specification gaps (total ratio of red to blue area) are 35.5% (one-step), 37.9% (large-area) and 34.1% (two-step) respectively.

completeness of parameter specification (see Figures S1 and S2, Supporting Information). In every case, the obtained correlation coefficients were below 0.25 indicating no significant correlation given the limited size of the dataset and the randomness of data selection. We conclude that, up to this point, the impact of a report is not linked to its completeness in specification of process paramters. Furthermore, there is no trend toward higher specification over time yet. By pointing out this open potential, we hope to see an improvement in the quality of experimental descriptions according to the here-provided guidelines in the future.

5. Conclusion and Outlook

Perovskite PVs have experienced immense improvements in device performance and stability within recent years. Researchers can be proud of initiating the innovative optimization process

of perovskite device fabrication. However, now that high industry adoption is projected, perovskite researchers working in academia should consider prioritizing fundamental analyses on perovskite processing through control and rigorous reporting over attempting to compete with industry on technological performance indicators. In this review, we shed light on the question of which process parameters impact perovskite morphology formation and thereby which conditions must be specified to achieve superior process reproducibility. We categorize common perovskite processes according to one-step or two-step routes and, as a subcategory, the involved mass transfer processes. Further, our overview survey on one- and two-step highly efficient devices as well as large-area perovskite devices demonstrates that there is already an implicit standard as to which parameters are reported by researchers. We propose that this standard should be extended by some additional, impactful parameters. A straight forward option is to use a scientific data management software systems implementing the thin-film solar cell ontology such as NOMAD. Furthermore, journals should consider requesting a mask of a minimum set of parameters to be provided for a work such as the table provided with this work. Lastly, we want to stress that these results also mirror the quality of reporting of our own publications and that closing the outlined specification gaps is a community effort.

We conclude that the completeness of the device fabrication section should be a priority in the future, as it is the most important resource for reproducing the results. Our structured table of parameters referenced to the perovskite ontology could be a first step in the right direction. In our view, we gave sufficient evidence for the need to control either of the presented parameters. Further, pilot studies have already shown the positive impact of automated parameters control. Better reporting and control of parameters will lead to more reproducibility for everyone involved in the device fabrication process, potentially saving large expenses in re-optimization. Device fabrication remains a multidimensional optimization problem. If one parameter is controlled or optimized, it does not mean that the determined optimal value will remain the ideal choice, when a different parameter changes. This fact underlines the great merit in enforcing completeness by standardizing and reporting process parameters in a machine-readable way. By increasing standardization, control and publishing of metadata, machine learning can leverage the available data to predict new fabrication guidelines from automated optimization. This can free up substantial financial and human resources that were previously devoted to re-optimizing parameter spaces. Further, the creation of digital twins is facilitated, and data can be reused more easily. To give a concrete example of implementation and industrial transferability, a research laboratory using smaller-scale table-top coating equipment can be connected to an ELN system storing their real-time device optimization parameters alongside key performance indicators in a database for exploration. These data can then be directly exploited in large-scale fabrication lines by enforcing similar process parameters in these larger coating and drying systems. Another application is in-line optimization of film properties from automated agents that have the proposed parameter table as an ontological knowledge base. Agents can further assist the laboratory workforce by giving new ideas or incentivize the execution of new experiments. They can also query operators to fill indisclose the required parameters of a successfully conducted experiment. We strongly encourage the community to establish a properly defined standard for the description of perovskite fabrication, ideally on the bases of the thin-film solar cell ontology, that extends beyond the implicit mimicking of top-cited reports. In addition to the specification of process parameters, optical and x-ray of intermediate and final film quality augment the control of perovskite solution processes. It is unclear whether or when scientific journals will require digitalization of experimental descriptions as a precondition for publication. We hope that this review marks a starting point for initiating a discussion on standardized, reproducible reporting of perovskite fabrication.

Supporting Information

Supporting Information is available from the Wiley Online Library or from the author.

Acknowledgements

S.T. acknowledges the European Union's Framework Programme for Research and Innovation Horizon Europe (2021-2027) under the Marie Skłodowska-Curie Grant Agreement No. 101107885 "INT-PVK-PRINT". L.A.C. acknowledges the European Union's Framework Programme for Research and Innovation Horizon Europe (2021-2027) under the Marie Sklodowska–Curie Grant Agreement No. 101068387 "EFESO"Author: Please check funding information and confirm its correctness. Many authors were part of the VIPERLAB Project funded from the European Union's Horizon 2020 research and innovation programme under grant agreement N°101006715. A part of this work has been supported by the Helmholtz Association in the framework of the Solar Technology Acceleration Platform (Solar TAP). Wei Yu is acknowledged for his help with the literature search. LUMINOSITY has received funding from the European Unions's Horizon Europe research and innovation programme under grant agreement no 101147653.

Open access publishing facilitated by Consiglio Nazionale delle Ricerche, as part of the Wiley - CRUI-CARE agreement.

Conflict of Interest

The authors declare no conflict of interest.

Keywords

automation, digital twin, perovskite photovoltaics, process parameters, reproducibility, standardization, thin film ontology

Received: June 11, 2025
Revised: August 15, 2025
Published online: October 3, 2025

[1] S. Liu, V. P. Biju, Y. Qi, W. Chen, Z. Liu, *NPG Asia Mater.* **2023**, *15*, 1.
[2] H. J. Snaith, *J. Phys. Chem. Lett.* **2013**, *4*, 3623.
[3] N. K. Elumalai, M. A. Mahmud, D. Wang, A. Uddin, *Energies* **2016**, *9*, 861.
[4] I. A. Howard, T. Abzieher, I. M. Hossain, H. Eggers, F. Schackmar, S. Ternes, B. S. Richards, U. Lemmer, U. W. Paetzold, *Adv. Mater.* **2019**, *31*, 1806702.
[5] K. X. Steirer, P. Schulz, G. Teeter, V. Stevanovic, M. Yang, K. Zhu, J. J. Berry, *ACS Energy Lett.* **2016**, *1*, 360.

[6] P. Brenner, T. Glöckler, D. Rueda-Delgado, T. Abzieher, M. Jakoby, B. S. Richards, U. W. Paetzold, I. A. Howard, U. Lemmer, *Opt. Mater. Express* **2017**, *7*, 4082.
[7] Z. Hu, Z. Lin, J. Su, J. Zhang, J. Chang, Y. Hao, *Sol. RRL* **2019**, *3*, 1900304.
[8] M. H. Miah, M. U. Khandaker, M. B. Rahman, M. Nur-E-Alam, M. A. Islam, *RSC Adv.* **2024**, *14*, 15876.
[9] W. Bai, T. Xuan, H. Zhao, H. Dong, X. Cheng, L. Wang, R. J. Xie, *Adv. Mater.* **2023**, *35*, 2302283.
[10] B. Zhao, B. Guo, S. Xing, Z. Liu, Y. Yuan, Z. Ren, W. Tang, Y. Lian, G. Zhang, C. Zou, D. Di, *Matter* **2024**, *7*, 772.
[11] Y. Sun, L. Ge, L. Dai, C. Cho, J. Ferrer Orri, K. Ji, S. J. Zelewski, Y. Liu, A. J. Mirabelli, Y. Zhang, J. Y. Huang, Y. Wang, K. Gong, M. C. Lai, L. Zhang, D. Yang, J. Lin, E. M. Tennyson, C. Ducati, S. D. Stranks, L. S. Cui, N. C. Greenham, *Nature* **2023**, *615*, 830.
[12] J. Song, Q. Shang, X. Deng, Y. Liang, C. Li, X. Liu, Q. Xiong, Q. Zhang, *Adv. Mater.* **2023**, *35*, 2302170.
[13] Q. Zhang, Q. Shang, R. Su, T. T. H. Do, Q. Xiong, *Nano Lett.* **2021**, *21*, 1903.
[14] I. Allegro, V. Bonal, E. R. Mamleyev, J. M. Villalvilla, J. A. Quintana, Q. Jin, M. A. Díaz-García, U. Lemmer, *ACS Appl. Mater. Interfaces* **2023**, *15*, 8436.
[15] K. Sakhatskyi, B. Turedi, G. J. Matt, E. Wu, A. Sakhatska, V. Bartosh, M. N. Lintangpradipto, R. Naphade, I. Shorubalko, O. F. Mohammed, S. Yakunin, O. M. Bakr, M. V. Kovalenko, *Nat. Photonics* **2023**, *17*, 510.
[16] J. Pang, H. Wu, H. Li, T. Jin, J. Tang, G. Niu, *Nat. Commun.* **2024**, *15*, 1.
[17] H. Mescher, F. Schackmar, H. Eggers, T. Abzieher, M. Zuber, E. Hamann, T. Baumbach, B. S. Richards, G. Hernandez-Sosa, U. W. Paetzold, U. Lemmer, *ACS Appl. Mater. Interfaces* **2020**, *12*, 15774.
[18] S. Hu, Z. Ren, A. B. Djurisic, A. L. Rogach, *ACS Energy Lett.* **2021**, *6*, 3882.
[19] Y. Zhou, J. Wang, D. Luo, D. Hu, Y. Min, Q. Xue, *Nano Energy* **2022**, *94*, 106949.
[20] F. Paulus, C. Tyznik, O. D. Jurchescu, Y. Vaynzof, F. Paulus, C. Tyznik, O. D. Jurchescu, Y. Vaynzof, *Adv. Funct. Mater.* **2021**, *31*, 2101029.
[21] A. Liu, H. Zhu, S. Bai, Y. Reo, T. Zou, M. G. Kim, Y. Y. Noh, *Nat. Electron.* **2022**, *5*, 78.
[22] F. Zhang, H. Zhang, L. Zhu, L. Qin, Y. Wang, Y. Hu, Z. Lou, Y. Hou, F. Teng, *J Mater Chem C Mater* **2019**, *7*, 4004.
[23] number of hits in the year 2024 when searching the term 'perovskite solar' on the lens, https://www.lens.org (accessed: June 2025).
[24] H. Zhu, S. Teale, M. N. Lintangpradipto, S. Mahesh, B. Chen, M. D. McGehee, E. H. Sargent, O. M. Bakr, *Nat. Rev. Mater.* **2023**, *8*, 569.
[25] "Interactive Best Research-Cell Efficiency Chart | Photovoltaic Research | NREL", can be found under, https://www.nrel.gov/pv/interactive-cell-efficiency.html (accessed: December 2025).
[26] O. Almora, G. C. Bazan, C. I. Cabrera, L. A. Castriotta, S. Erten-Ela, K. Forberich, K. Fukuda, F. Guo, J. Hauch, A. W. Y. Ho-Baillie, T. J. Jacobsson, R. A. J. Janssen, T. Kirchartz, R. R. Lunt, X. Mathew, D. B. Mitzi, M. K. Nazeeruddin, J. Nelson, A. F. Nogueira, U. W. Paetzold, B. P. Rand, U. Rau, T. Someya, C. Sprau, L. Vaillant-Roca, C. J. Brabec, *Adv. Energy Mater.* **2025**, *15*, 2404386.
[27] M. Peplow, *Nature* **2023**, *623*, 902.
[28] "Perovskite Solar Cells Module Market Size | CAGR of 54.9%", can be found under, https://market.us/report/perovskite-solar-cells-module-market/ (accessed: July 2024).
[29] "Commercial perovskites imminent – pv magazine International", can be found under, https://www.pv-magazine.com/2023/10/31/commercial-perovskites-imminent/ (accessed: July 2024).
[30] Solar Power Europe, Global Market Outlook **2025**, https://www.solarpowereurope.org/insights/outlooks/global-market-outlook-for-solar-power-2025-2029/detail#executive-summary (accessed: September 2025).
[31] "Weekend read: Perovskites move into production – pv magazine Australia", can be found under, https://www.pv-magazine-australia.com/2024/05/18/weekend-read-perovskites-move-into-production/ (accessed: July 2024).
[32] "Perovskite solar goes commercial as yield gains align with market forces | Reuters", can be found under, https://www.reuters.com/business/energy/perovskite-solar-goes-commercial-yield-gains-align-with-market-forces-2023-02-02/ (accessed: July 2024).
[33] "Global Perovskite Solar Cells Industry Research Report 2023 Competitive Landscape Market – Industry Reports", can be found under, https://www.researchreportsworld.com/global-perovskite-solar-cells-industry-research-report-2023-competitive-landscape-market-22356880 (accessed: July 2024).
[34] "Oxford PV starts commercial distribution of perovskite solar modules – pv magazine International", can be found under, https://www.pv-magazine.com/2024/09/05/oxford-pv-starts-commercial-distribution-of-perovskite-solar-modules/ (accessed: May 2025).
[35] P. Holzhey, M. Prettl, S. Collavini, N. L. Chang, M. Saliba, *Joule* **2023**, *7*, 257.
[36] L. A. Zafoschnig, S. Nold, J. C. Goldschmidt, *IEEE J Photovolt* **2020**, *10*, 1632.
[37] S. E. Sofia, H. Wang, A. Bruno, J. L. Cruz-Campa, T. Buonassisi, I. M. Peters, *Sustain Energy Fuels* **2020**, *4*, 852.
[38] **N.d**, Perovskites move into production – pv magazine USA, https://pv-magazine-usa.com/2024/05/24/perovskites-move-into-production/ (accessed: July 2024).
[39] "Chinese PV Industry Brief: PowerChina signs 1.05 GW Terra solar deal – pv magazine International", can be found under, https://www.pv-magazine.com/2024/12/03/chinese-pv-industry-brief-powerchina-signs-1-05-gw-terra-solar-deal/ (accessed: May 2025).
[40] "Chinese PV Industry Brief: UtmoLight starts perosvkite module production – pv magazine International", can be found under, https://www.pv-magazine.com/2025/02/07/chinese-pv-industry-brief-utmolight-begins-perosvkite-solar-module-production-at-gw-scale-facility/ (accessed: May 2025).
[41] J. S. Yeo, Y. Jeong, *Energy Reports* **2020**, *6*, 2075.
[42] V. Larini, L. Ardito, A. Messeni Petruzzelli, F. Matteucci, G. Grancini, *Chem* **2023**, *9*, 2738.
[43] J. Han, K. Park, S. Tan, Y. Vaynzof, J. Xue, E. W. G. Diau, M. G. Bawendi, J. W. Lee, I. Jeon, *Nature Reviews Methods Primers* **2025**, *5*, 1.
[44] A. Agresti, F. Di Giacomo, S. Pescetelli, A. Di Carlo, *Nano Energy* **2024**, *122*, 109317.
[45] R. Liu, K. Xu, *Micro Nano Lett* **2020**, *15*, 349.
[46] L. Gu, F. Fei, Y. Xu, S. Wang, N. Yuan, J. Ding, *ACS Appl. Mater. Interfaces* **2022**, *14*, 2949.
[47] Y. Yu, F. Zhang, T. Hou, X. Sun, H. Yu, M. Zhang, *Sol. RRL* **2021**, *5*, 2100386.
[48] M. Saliba, T. Matsui, J. Y. Seo, K. Domanski, J. P. Correa-Baena, M. K. Nazeeruddin, S. M. Zakeeruddin, W. Tress, A. Abate, A. Hagfeldt, M. Grätzel, *Energy Environ. Sci.* **2016**, *9*, 1989.
[49] D. P. McMeekin, G. Sadoughi, W. Rehman, G. E. Eperon, M. Saliba, M. T. Horantner, A. Haghighirad, N. Sakai, L. Korte, B. Rech, M. B. Johnston, L. M. Herz, H. J. Snaith, *Science* **2016**, *351*, 151.
[50] Z. Liang, Y. Zhang, H. Xu, W. Chen, B. Liu, J. Zhang, H. Zhang, Z. Wang, D. H. Kang, J. Zeng, X. Gao, Q. Wang, H. Hu, H. Zhou, X. Cai, X. Tian, P. Reiss, B. Xu, T. Kirchartz, Z. Xiao, S. Dai, N. G. Park, J. Ye, X. Pan, *Nature* **2023**, *624*, 557.
[51] X. Li, J. M. Hoffman, M. G. Kanatzidis, *Chem. Rev.* **2021**, *121*, 2230.

[52] T. L. Leung, I. Ahmad, A. A. Syed, A. M. C. Ng, J. Popović, A. B. Djurišić, *Commun. Mater.* **2022**, *3*, 63.
[53] X. Zheng, W. Kong, J. Wen, J. Hong, H. Luo, R. Xia, Z. Huang, X. Luo, Z. Liu, H. Li, H. Sun, Y. Wang, C. Liu, P. Wu, H. Gao, M. Li, A. D. Bui, Y. Mo, X. Zhang, G. Yang, Y. Chen, Z. Feng, H. T. Nguyen, R. Lin, L. Li, J. Gao, H. Tan, *Nat. Commun.* **2024**, *15*, 4907.
[54] J. Jiao, C. Yang, Z. Wang, C. Yan, C. Fang, *Results in Engineering* **2023**, *18*, 101158.
[55] B. M. Gallant, P. Holzhey, J. A. Smith, S. Choudhary, K. A. Elmestekawy, P. Caprioglio, I. Levine, A. A. Sheader, E. Y.-H. Hung, F. Yang, D. T. W. Toolan, R. C. Kilbride, K.-A. Zaininger, J. M. Ball, M. G. Christoforo, N. K. Noel, L. M. Herz, D. J. Kubicki, H. J. Snaith, *Nat. Commun.* **2024**, *15*, 10110.
[56] H. Zhang, K. Darabi, N. Y. Nia, A. Krishna, P. Ahlawat, B. Guo, M. H. S. Almalki, T. Sen Su, D. Ren, V. Bolnykh, L. A. Castriotta, M. Zendehdel, L. Pan, S. S. Alonso, R. Li, S. M. Zakeeruddin, A. Hagfeldt, U. Rothlisberger, A. Di Carlo, A. Amassian, M. Grätzel, *Nat. Commun.* **2022**, *13*, 89.
[57] Y. Duan, Y. Chen, Y. Wu, Z. Liu, S. Liu, Q. Peng, *Adv. Funct. Mater.* **2024**, *34*, 2315604.
[58] S. Foo, M. Thambidurai, P. Senthil Kumar, R. Yuvakkumar, Y. Huang, C. Dang, *Int. J. Energy Res.* **2022**, *46*, 21441.
[59] P. Zhao, B. J. Kim, H. S. Jung, *Mater. Today Energy* **2018**, *7*, 267.
[60] Z. Zhang, L. Qiao, K. Meng, R. Long, G. Chen, P. Gao, *Chem. Soc. Rev.* **2023**, *52*, 163.
[61] Q. Jiang, Y. Zhao, X. Zhang, X. Yang, Y. Chen, Z. Chu, Q. Ye, X. Li, Z. Yin, J. You, *Nat. Photonics* **2019**, *13*, 460.
[62] S. Liu, Y. Guan, Y. Sheng, Y. Hu, Y. Rong, A. Mei, H. Han, *Adv. Energy Mater.* **2020**, *10*, 1902492.
[63] A. Mahapatra, D. Prochowicz, M. M. Tavakoli, S. Trivedi, P. Kumar, P. Yadav, *J Mater Chem A Mater* **2019**, *8*, 27.
[64] B. Ding, Y. Ding, J. Peng, J. Romano-deGea, L. E. K. Frederiksen, H. Kanda, O. A. Syzgantseva, M. A. Syzgantseva, J. N. Audinot, J. Bour, S. Zhang, T. Wirtz, Z. Fei, P. Dörflinger, N. Shibayama, Y. Niu, S. Hu, S. Zhang, F. F. Tirani, Y. Liu, G. J. Yang, K. Brooks, L. Hu, S. Kinge, V. Dyakonov, X. Zhang, S. Dai, P. J. Dyson, M. K. Nazeeruddin, *Nature* **2024**, *628*, 299.
[65] K. Forberich, S. Albrecht, L. A. Castriotta, A. Distler, J. Hauch, T. Kirchartz, U. W. Paetzold, S. Schorr, C. Sprau, B. Stannowski, S. Ternes, E. Unger, T. Unold, C. J. Brabec, *Adv. Energy Mater.* **2024**, *15*, 2404036.
[66] A. Giuri, R. Mastria, A. Rizzo, *Cell Rep Phys Sci* **2024**, *5*, 102245.
[67] T. D. Siegler, A. Dawson, P. Lobaccaro, D. Ung, M. E. Beck, G. Nilsen, L. L. Tinker, *ACS Energy Lett.* **2022**, *7*, 1728.
[68] J. A. Christians, J. S. Manser, P. V. Kamat, *J. Phys. Chem. Lett.* **2015**, *6*, 852.
[69] S. H. Jeong, J. Park, T. H. Han, F. Zhang, K. Zhu, J. S. Kim, M. H. Park, M. O. Reese, S. Yoo, T. W. Lee, *Joule* **2020**, *4*, 1206.
[70] W. Tress, *Adv. Energy Mater.* **2017**, *7*, 1602358.
[71] W. Tress, M. Yavari, K. Domanski, P. Yadav, B. Niesen, J. P. Correa Baena, A. Hagfeldt, M. Graetzel, *Energy Environ. Sci.* **2018**, *11*, 151.
[72] M. V. Khenkin, E. A. Katz, A. Abate, G. Bardizza, J. J. Berry, C. Brabec, F. Brunetti, V. Bulović, Q. Burlingame, A. Di Carlo, R. Cheacharoen, Y. B. Cheng, A. Colsmann, S. Cros, K. Domanski, M. Dusza, C. J. Fell, S. R. Forrest, Y. Galagan, D. Di Girolamo, M. Grätzel, A. Hagfeldt, E. von Hauff, H. Hoppe, J. Kettle, H. Köbler, M. S. Leite, S. (Frank) Liu, Y. L. Loo, J. M. Luther, et al., *Nat. Energy* **2020**, *5*, 35.
[73] Y. Zhou, L. M. Herz, A. K. Y. Jen, M. Saliba, *Nat. Energy* **2022**, *7*, 794.
[74] M. Saliba, J. P. Correa-Baena, C. M. Wolff, M. Stolterfoht, N. Phung, S. Albrecht, D. Neher, A. Abate, *Chem. Mater.* **2018**, *30*, 4193.
[75] F W. Liou, *Rapid Prototyping And Engineering Applications: A Toolbox for Prototype Development*, CRC Press Inc, Boca Raton, **2007**.
[76] K. P. Goetz, Y. Vaynzof, *ACS Energy Lett.* **2022**, 1750.
[77] More important examples of frequently occurring synonyms can be found in Table S1, which maps the terms used herein to other commonly employed terminology.
[78] "IEC TR 63228:2019 | IEC", can be found under, https://webstore.iec.ch/en/publication/64040 (accessed: July 2024).
[79] M. Saliba, M. Stolterfoht, C. M. Wolff, D. Neher, A. Abate, *Joule* **2018**, *2*, 1019.
[80] "Thin-film solar cell ontology – Summary | Materials Open Laboratory MatPortal", can be found under, https://matportal.org/ontologies/TFSCO (accessed: May 2025).
[81] J. Zhang, V. M. Le Corre, J. Wu, T. Du, T. Osterrieder, K. Zhang, H. Zhang, L. Lüer, J. Hauch, C. J. Brabec, *Adv. Energy Mater.* **2025**, *15*, 2404957.
[82] J. Zhang, J. Wu, A. Barabash, T. Du, S. Qiu, V. M. Le Corre, Y. Zhao, K. Zhang, F. Schmitt, Z. Peng, J. Tian, C. Li, C. Liu, T. Heumueller, L. Luer, J. A. Hauch, C. J. Brabec, *Energy Environ. Sci.* **2024**, *17*, 5490.
[83] D. O. Baumann, F. Laufer, J. Roger, R. Singh, M. Gholipoor, U. W. Paetzold, *ACS Appl. Mater. Interfaces* **2024**, *16*, 54007.
[84] J. Wagner, C. G. Berger, X. Du, T. Stubhan, J. A. Hauch, C. J. Brabec, *J. Mater. Sci.* **2021**, *56*, 16422.
[85] M. A. Reus, T. Baier, C. G. Lindenmeir, A. F. Weinzierl, A. Buyan-Arivjikh, S. A. Wegener, D. P. Kosbahn, L. K. Reb, J. Rubeck, M. Schwartzkopf, S. V. Roth, P. Müller-Buschbaum, *Rev. Sci. Instrum.* **2024**, *95*, 43907.
[86] X. Li, G. Nasti, C. Dreessen, J. Dagar, R. Meitzner, D. Amoroso, P. L. Maffettone, T. Kirchartz, E. Unger, A. Abate, S. D. Dimitrov, *Sustain Energy Fuels* **2025**, *9*, 2063.
[87] S. Qiu, M. Majewski, L. Dong, D. Jang, V. M. L. Corre, J. G. Cerrillo, O. J. J. Ronsin, F. Yang, F. Guo, K. Zhang, L. Lüer, J. Harting, T. Du, C. J. Brabec, H. J. Egelhaaf, *Adv. Energy Mater.* **2024**, *14*, 2303210.
[88] S. Ternes, F. Laufer, P. Scharfer, W. Schabel, B. S. Richards, I. A. Howard, U. W. Paetzold, *Sol. RRL* **2021**, *6*, 2100353.
[89] S. Biberger, M. Spies, K. Schötz, F. J. Kahle, N. Leupold, R. Moos, H. Grüninger, A. Köhler, F. Panzer, *J Mater Chem C Mater* **2024**, *12*, 6415.
[90] J. Zhang, B. Liu, Z. Liu, J. Wu, S. Arnold, H. Shi, T. Osterrieder, J. A. Hauch, Z. Wu, J. Luo, J. Wagner, C. G. Berger, T. Stubhan, F. Schmitt, K. Zhang, M. Sytnyk, T. Heumueller, C. M. Sutter-Fella, I. M. Peters, Y. Zhao, C. J. Brabec, *Adv. Energy Mater.* **2023**, *13*, 2302594.
[91] F. Laufer, M. Götz, U. W. Paetzold, *Energy Environ. Sci.* **2025**, *18*, 1767.
[92] URIs are, in essence, unique names for the same conceptual entities that can be leveraged for conducting data-driven meta-analyses on perovskite processing, later on.
[93] L. Lüer, I. M. Peters, A. S. Smith, E. Dorschky, B. M. Eskofier, F. Liers, J. Franke, M. Sjarov, M. Brossog, D. M. Guldi, A. Maier, C. J. Brabec, *Joule* **2024**, *8*, 295.
[94] We focus on process parameters that are general enough to apply for the vast majority of solution processes and thus exclude parameters of high specificity and variability in occurrence, such as coating technique-related and material-related parameters, but the standard can be extended, later on. These specific parameters are summarized with generalizing terms such as "coating parameters" or "composition of solution".
[95] T. J. Jacobsson, A. Hultqvist, A. García-Fernández, A. Anand, A. Al-Ashouri, A. Hagfeldt, A. Crovetto, A. Abate, A. G. Ricciardulli, A. Vijayan, A. Kulkarni, A. Y. Anderson, B. P. Darwich, B. Yang, B. L. Coles, C. A. R. Perini, C. Rehermann, D. Ramirez, D. Fairen-Jimenez, D. Di Girolamo, D. Jia, E. Avila, E. J. Juarez-Perez, F. Baumann, F. Mathies, G. S. A. González, G. Boschloo, G. Nasti, G. Paramasivam, G. Martínez-Denegri, et al., *Nat. Energy* **2021**, *7*, 107.
[96] K. R. Hansen, L. Whittaker-Brooks, *Matter* **2022**, *5*, 2461.
[97] These range from Electronic Laboratory Notebook (ELN) systems, such as elabFTW, openBIS, chemotion (all open source) and

labfolder (commercial), toward systems that include repositories and data publishing such as the open source data repository scicat (see also, https://eln-finder.ulb.tu-darmstadt.de/home for other ELNs). As an alternative to the afore-mentioned solution, the open source software NOMAD is a particularly compelling tool for public research institutions. Originally dedicated for simulated data it became part of the NFDI (German research data infrastructure initiative) project FAIRmat (https://www.fairmat-nfdi.eu/fairmat/), where it is further developed and extended to experimental material science data. NOMAD allows research labs to digitalize their workflows, structure their data, integrate custom analysis and publish data together with the analysis. It is thus more than an ELN, since it does not only document scientific work digitally, but it also allows to integrate data standards such as NeXus and Ontologies/Vocabularies such as the TFSCO to contribute to more reusable and interoperable data publications.

[98] Y. Vaynzof, *Adv. Energy Mater.* **2020**, *10*, 2003073.
[99] Z. Saki, M. M. Byranvand, N. Taghavinia, M. Kedia, M. Saliba, *Energy Environ. Sci.* **2021**, *14*, 5690.
[100] A. Kojima, K. Teshima, Y. Shirai, T. Miyasaka, *J. Am. Chem. Soc.* **2009**, *131*, 6050.
[101] F. Di Giacomo, V. Zardetto, G. Lucarelli, L. Cinà, A. Di Carlo, M. Creatore, T. M. Brown, *Nano Energy* **2016**, *30*, 460.
[102] F. Cao, L. Bian, L. Li, *Energy Materials and Devices* **2024**, *2*, 9370018.
[103] D. Bi, S. J. Moon, L. Häggman, G. Boschloo, L. Yang, E. M. J. Johansson, M. K. Nazeeruddin, M. Grätzel, A. Hagfeldt, *RSC Adv.* **2013**, *3*, 18762.
[104] S. Ternes, F. Laufer, U. W. Paetzold, S. Ternes, F. Laufer, U. W. Paetzold, *Adv. Sci.* **2024**, *11*, 2308901.
[105] L. Zeng, S. Chen, K. Forberich, C. J. Brabec, Y. Mai, F. Guo, *Energy Environ. Sci.* **2020**, *13*, 4666.
[106] J. Muir, *Proc. Royal Soc. London* **1903**, *71*, 80.
[107] C. A. Edwards, *Trans. Faraday Soc.* **1915**, *10*, 248.
[108] K. Hwang, Y.-S. Jung, Y.-J. Heo, F. H. Scholes, S. E. Watkins, J. Subbiah, D. J. Jones, D.-Y. Kim, D. Vak, K. Hwang, Y. Jung, Y. Heo, D. Kim, F. H. Scholes, S. E. Watkins, D. Vak, J. Subbiah, D. J. Jones, *Adv. Mater.* **2015**, *27*, 1241.
[109] S. Ternes, *In Situ Characterization and Modelling of Drying Dynamics for Scalable Printing of Hybrid Perovskite Photovoltaics*, KIT Scientific Publishing, Karlsruhe, Germany **2023**, ISBN978-3-7315-1255-4
[110] B. Schmidt-Hansberg, H. Do, A. Colsmann, U. Lemmer, W. Schabel, *Eur. Phys. J.: Special Topics* **2009**, *166*, 49.
[111] M. Kohlstädt, M. A. Yakoob, U. Würfel, *Phys. Status Solidi (A) Appl. Mater. Sci.* **2018**, *215*, 1.
[112] H. Kautsky, *Trans. Faraday Soc.* **1939**, *35*, 216.
[113] R. Cheng, C.-C. Chung, H. Zhang, Z. Zhou, P. Zhai, Y.-T. Huang, H. Lee, S.-P. Feng, *Small* **2019**, *15*, 1804465.
[114] L. Gao, K. Huang, C. Long, F. Zeng, B. Liu, J. Yang, *Appl Phys A Mater Sci Process* **2020**, *126*, 452.
[115] M. Majewski, S. Qiu, O. Ronsin, L. Lü er, V. M. Le Corre, T. Du, bc C. J. Brabec, bc H-J. Egelhaaf bc, J. Harting ad, *Mater. Horiz.* **2025**, *12*, 555.
[116] Supersaturation is defined as the logarithm of the ratio of the solute concentration and the equilibrium concentration of the crystallized-dissolved phase equilibrium.
[117] S. Ternes, J. Mohacsi, N. Lüdtke, H. M. Pham, M. Arslan, P. Scharfer, W. Schabel, B. S. Richards, U. W. Paetzold, *ACS Appl. Mater. Interfaces* **2022**, *14*, 11300.
[118] L. Wang, G. Liu, X. Xi, G. Yang, L. Hu, B. Zhu, Y. He, Y. Liu, H. Qian, S. Zhang, H. Zai, *Crystals* **2022**, *12*, 894.
[119] A. H. Ghahremani, B. Martin, A. Gupta, J. Bahadur, K. Ankireddy, T. Druffel, *Mater. Des.* **2020**, *185*, 108237.
[120] K. Bruening, B. Dou, J. Simonaitis, Y. Y. Lin, M. F. A. M. van Hest, C. J. Tassone, *Joule* **2018**, *2*, 2464.
[121] Z. Ouyang, M. Yang, J. B. Whitaker, D. Li, M. F. A. M. Van Hest, *ACS Appl. Energy Mater.* **2020**, *3*, 3714.
[122] L. A. Castriotta, F. Matteocci, L. Vesce, L. Cinà, A. Agresti, S. Pescetelli, A. Ronconi, M. Löffler, M. M. Stylianakis, F. Di Giacomo, P. Mariani, M. Stefanelli, E. M. Speller, A. Alfano, B. Paci, A. Generosi, F. Di Fonzo, A. Petrozza, B. Rellinghaus, E. Kymakis, A. Di Carlo, *ACS Appl. Mater. Interfaces* **2021**, *13*, 11741.
[123] S. Sanchez, X. Hua, N. Phung, U. Steiner, A. Abate, *Adv. Energy Mater.* **2018**, *8*, 1702915.
[124] L. Wagner, S. Mastroianni, A. Hinsch, *Joule* **2020**, *4*, 882.
[125] F. P. Incropera, D. P. DeWitt, T. L. Bergmann, A. S. Lavine, *Fundamentals of Heat and Mass Transfer*, 6th ed., John Wiley And Sons Inc., New York, **2006**.
[126] N. J. Jeon, J. H. Noh, Y. C. Kim, W. S. Yang, S. Ryu, S. Il Seok, *Nat. Mater.* **2014**, *13*, 897.
[127] L. Vesce, M. Stefanelli, J. P. Herterich, L. A. Castriotta, M. Kohlstädt, U. Würfel, A. Di Carlo, *Sol. RRL* **2021**, *5*, 2100073.
[128] E. Calabrò, F. Matteocci, A. L. Palma, L. Vesce, B. Taheri, L. Carlini, I. Pis, S. Nappini, J. Dagar, C. Battocchio, T. M. Brown, A. Di Carlo, *Sol. Energy Mater. Sol. Cells* **2018**, *185*, 136.
[129] F. Matteocci, L. Vesce, F. U. Kosasih, L. A. Castriotta, S. Cacovich, A. L. Palma, G. Divitini, C. Ducati, A. Di Carlo, *ACS Appl. Mater. Interfaces* **2019**, *11*, 25195.
[130] M. Azhar, Y. Yalcinkaya, D. T. Cuzzupè, Y. Abebe Temitmie, M. I. Haider, L. Schmidt-Mende, **2025**, *1*, 5.
[131] K. Geistert, S. Ternes, D. B. Ritzer, U. W. Paetzold, *ACS Appl. Mater. Interfaces* **2023**, *15*, 52519.
[132] The Reynolds number of a moving fluid represents the ratio of inertial to viscous forces. It is defined as $Re_x = u_0\, x/\nu$, where u_0[m/s] is the velocity of the fluid, x[m/s] is a characteristic length scale of the flow and ν[m/s^2] is the kinematic viscosity of the fluid. The Reynolds number can be defined for impinging jets and linear flows. For typical parameters used in perovskite processing, one obtains the approximate range $100 < Re_x < 100,000$, where flows with $Re_x < 2000$ are commonly laminar and flows $Re_x > 3000$ turbulent. We note that the Reynolds number is proportional to gas pressure, $Re_x \propto p_{Gas}$, which implies that the lower boundary does not apply in vacuum-assisted methods and laminar air flow is much more likely to occur.
[133] S. Ternes, T. Börnhorst, J. A. Schwenzer, I. M. Hossain, T. Abzieher, W. Mehlmann, U. Lemmer, P. Scharfer, W. Schabel, B. S. Richards, U. W. Paetzold, *Adv. Energy Mater.* **2019**, *9*, 1901581.
[134] L. L. Gao, K. J. Zhang, N. Chen, G. J. Yang, *J Mater Chem A Mater* **2017**, *5*, 18120.
[135] F. Mathies, H. Eggers, B. S. Richards, G. Hernandez-Sosa, U. Lemmer, U. W. Paetzold, *ACS Appl. Energy Mater.* **2018**, *1*, 1834.
[136] S. Schlisske, F. Mathies, D. Busko, N. Strobel, T. Rödlmeier, B. S. Richards, U. Lemmer, U. W. Paetzold, G. Hernandez-Sosa, E. Klampaftis, *ACS Appl. Energy Mater.* **2019**, *2*, 764.
[137] F. Schackmar, F. Laufer, R. Singh, A. Farag, H. Eggers, S. Gharibzadeh, B. Abdollahi Nejand, U. Lemmer, G. Hernandez-Sosa, U. W. Paetzold, *Adv. Mater. Technol.* **2023**, *8*, 2201331.
[138] F. Mathies, T. Abzieher, A. Hochstuhl, K. Glaser, A. Colsmann, U. W. W. Paetzold, G. Hernandez-Sosa, U. Lemmer, A. Quintilla, *J Mater Chem A Mater* **2016**, *4*, 19207.
[139] F. Mathies, E. R. Nandayapa, G. Paramasivam, M. F. Al Rayes, V. R. F. Schröder, C. Rehermann, E. J. W. List-Kratochvil, E. L. Unger, *Mater. Adv.* **2021**, *2*, 5365.
[140] H. Hu, D. B. Ritzer, A. Diercks, Y. Li, R. Singh, P. Fassl, Q. Jin, F. Schackmar, U. W. Paetzold, B. A. Nejand, *Joule* **2023**, *7*, 1574.
[141] B. Abdollahi Nejand, D. B. Ritzer, H. Hu, F. Schackmar, S. Moghadamzadeh, T. Feeney, R. Singh, F. Laufer, R. Schmager, R.

Azmi, M. Kaiser, T. Abzieher, S. Gharibzadeh, E. Ahlswede, U. Lemmer, B. S. Richards, U. W. Paetzold, *Nat. Energy* **2022**, *7*, 620.
[142] B. Abdollahi Nejand, I. M. Hossain, M. Jakoby, S. Moghadamzadeh, T. Abzieher, S. Gharibzadeh, J. A. Schwenzer, P. Nazari, F. Schackmar, D. Hauschild, L. Weinhardt, U. Lemmer, B. S. Richards, I. A. Howard, U. W. Paetzold, *Adv. Energy Mater.* **2019**, *10*, 1902583.
[143] B. Schmidt-Hansberg, M. Baunach, J. Krenn, S. Walheim, U. Lemmer, P. Scharfer, W. Schabel, *Chem. Eng. Proc.: Process Intensification* **2011**, *50*, 509.
[144] D. S. Ham, W. J. Choi, H. Yun, M. Kim, D. H. Yeo, S. Lee, B. J. Kim, J. H. Lee, *ACS Appl. Energy Mater.* **2021**, *4*, 7611.
[145] B. Dollet, F. Boulogne, *Phys Rev Fluids* **2017**, *2*, 053501.
[146] Y. Fan, Y. Zhao, J. F. Torres, F. Xu, C. Lei, Y. Li, J. Carmeliet, *Phys. Fluids* **2021**, *33*, 101301.
[147] T. L. Bergman, F. P. Incropera, *Fundamentals of Heat and Mass Transfer*, Wiley, New Jersey, **2011**.
[148] C. Zuo, L. Tan, H. Dong, J. Chen, F. Hao, C. Yi, L. Ding, *DeCarbon* **2023**, *2*, 100020.
[149] Q. Chen, T. Ma, F. Wang, Y. Liu, S. Liu, J. Wang, Z. Cheng, Q. Chang, R. Yang, W. Huang, L. Wang, T. Qin, W. Huang, *Adv. Sci.* **2020**, *7*, 2000480.
[150] S. Sánchez, J. Jerónimo-Rendon, M. Saliba, A. Hagfeldt, *Mater. Today* **2020**, *35*, 9.
[151] N. Rolston, A. Sleugh, J. P. Chen, O. Zhao, T. W. Colburn, A. C. Flick, R. H. Dauskardt, *Front. Energy Res.* **2021**, *9*, 264.
[152] P. S. V. Ling, A. Hagfeldt, S. Sanchez, *JoVE (Journal of Visualized Experiments)* **2021**, *2021*, 61730.
[153] S. Tan, C. Li, C. Peng, W. Yan, H. Bu, H. Jiang, F. Yue, L. Zhang, H. Gao, Z. Zhou, *Nat. Commun.* **2024**, *15*, 1.
[154] S. Bhandari, A. Roy, A. Ghosh, T. K. Mallick, S. Sundaram, *Sustain Energy Fuels* **2020**, *4*, 6283.
[155] Y. Han, H. Xie, E. L. Lim, D. Bi, *Sol. RRL* **2022**, *6*, 2101007.
[156] J. Schlipf, P. Docampo, C. J. Schaffer, V. Körstgens, L. Bießmann, F. Hanusch, N. Giesbrecht, S. Bernstorff, T. Bein, P. Müller-Buschbaum, *J. Phys. Chem. Lett.* **2015**, *6*, 1265.
[157] M. Perez, S. S. Peled, T. Templeman, A. Osherov, V. Bulovic, E. A. Katz, Y. Golan, *Thin Solid Films* **2020**, *714*, 138367.
[158] Z. Wu, E. Bi, C. Li, L. Chen, Z. Song, Y. Yan, *Sol. RRL* **2023**, *7*, 2200571.
[159] S. R. Raga, L. K. Ono, Y. Qi, *J. Mater. Chem. A* **2016**, *4*, 2494.
[160] F. U. Kosasih, E. Erdenebileg, N. Mathews, S. G. Mhaisalkar, A. Bruno, *Joule* **2022**, *6*, 2692.
[161] K. Geistert, R. Pappenberger, P. Scharfer, P. Cavadini, W. Schabel, F. Sadegh, D. B. Ritzer, B. A. Nejand, U. W. Paetzold, K. Geistert, R. Pappenberger, F. Sadegh, D. B. Ritzer, U. W. Paetzold, P. Scharfer, P. Cavadini, W. Schabel, B. Abdollahi, N. M. Burger, *Adv. Energy Mater.* **2025**, *15*, 2500923.
[162] F. Jafarzadeh, L. A. Castriotta, E. Calabrò, P. Spinelli, A. Generosi, B. Paci, D. Becerril Rodriguez, M. Luce, A. Cricenti, F. Di Giacomo, F. Matteocci, F. Brunetti, A. Di Carlo, *Commun. Mater.* **2024**, *5*, 186.
[163] B. Chen, P. Wang, R. Li, N. Ren, W. Han, Z. Zhu, J. Wang, S. Wang, B. Shi, J. Liu, P. Liu, Q. Huang, S. Xu, Y. Zhao, X. Zhang, *ACS Energy Lett.* **2022**, *7*, 2771.
[164] R. Pappenberger, A. Diercks, J. Petry, S. Moghadamzadeh, P. Fassl, U. W. Paetzold, *Adv. Funct. Mater.* **2024**, *34*, 2311424.
[165] M. F. Mohamad Noh, N. A. Arzaee, I. N. Nawas Mumthas, A. Aadenan, H. Alessa, M. N. Alghamdi, H. Moria, N. A. Mohamed, A. R. Bin Mohd Yusoff, M. A. M. Teridi, *Electrochim. Acta* **2022**, *402*, 139530.
[166] S. Ahn, W. H. Chiu, H. M. Cheng, V. Suryanarayanan, G. Chen, Y. C. Huang, M. C. Wu, K. M. Lee, *Org. Electron.* **2023**, *120*, 106847.
[167] J. Cao, F. Wang, H. Yu, Y. Zhou, H. Lu, N. Zhao, C. P. Wong, *J Mater Chem A Mater* **2016**, *4*, 10223.
[168] R. Pesch, A. Diercks, J. Petry, A. Welle, R. Pappenberger, F. Schackmar, H. Eggers, J. Sutter, U. Lemmer, U. W. Paetzold, *Sol. RRL* **2024**, *8*, 2400165.
[169] K. Hwang, Y. S. Jung, Y. J. Heo, F. H. Scholes, S. E. Watkins, J. Subbiah, D. J. Jones, D. Y. Kim, D. Vak, *Adv. Mater.* **2015**, *27*, 1241.
[170] S. Raj Mohan, R. Das, T. S. Dhami, P. Gupta, R. Singh, S. K. Rai, M. P. Joshi, *Opt Mater (Amst)* **2024**, *147*, 114720.
[171] P. Ahlawat, A. Hinderhofer, E. A. Alharbi, H. Lu, A. Ummadisingu, H. Niu, M. Invernizzi, S. M. Zakeeruddin, M. I. Dar, F. Schreiber, A. Hagfeldt, M. Grätzel, U. Rothlisberger, M. Parrinello, *Sci. Adv.* **2021**, *7*, 3326.
[172] Z. Zhang, Y. Liu, P. Zhang, Y. Mao, *Org. Electron.* **2021**, *88*, 106007.
[173] A. Senocrate, T. Acartürk, G. Y. Kim, R. Merkle, U. Starke, M. Grätzel, J. Maier, *J Mater Chem A Mater* **2018**, *6*, 10847.
[174] Z. Hu, Z. Liu, L. K. Ono, M. Jiang, S. He, D. Y. Son, Y. Qi, *Adv. Energy Mater.* **2020**, *10*, 2000908.
[175] S. Pathak, A. Sepe, A. Sadhanala, F. Deschler, A. Haghighirad, N. Sakai, K. C. Goedel, S. D. Stranks, N. Noel, M. Price, S. Hüttner, N. A. Hawkins, R. H. Friend, U. Steiner, H. J. Snaith, *ACS Nano* **2015**, *9*, 2311.
[176] H. H. Huang, Z. Ma, J. Strzalka, Y. Ren, K. F. Lin, L. Wang, H. Zhou, Z. Jiang, W. Chen, *Cell Rep Phys Sci* **2021**, *2*, 100395.
[177] B. Jeong, S. M. Cho, S. H. Cho, J. H. Lee, I. Hwang, S. K. Hwang, J. Cho, T. W. Lee, C. Park, *physica status solidi (RRL) – Rapid Research Letters* **2016**, *10*, 381.
[178] J. Li, A. Dobrovolsky, A. Merdasa, E. L. Unger, I. G. Scheblykin, *ACS Omega* **2018**, *3*, 14494.
[179] S. W. Kim, S. J. Moon, S. H. Kim, J. J. Yoo, D. Kim, B. S. Kim, N. J. Jeon, *ACS Energy Lett.* **2023**, *8*, 4777.
[180] M. K. Gangishetty, R. W. J. Scott, T. L. Kelly, *Nanoscale* **2016**, *8*, 6300.
[181] K. Liu, Y. Luo, Y. Jin, T. Liu, Y. Liang, L. Yang, P. Song, Z. Liu, C. Tian, L. Xie, Z. Wei, *Nat. Commun.* **2022**, *13*, 1.
[182] J. You, Z. Hong, T. Bin Song, L. Meng, Y. Liu, C. Jiang, H. Zhou, W. H. Chang, G. Li, Y. Yang, *Appl. Phys. Lett.* **2014**, *703*, 105.
[183] J. Liu, C. Gao, X. He, Q. Ye, L. Ouyang, D. Zhuang, C. Liao, J. Mei, W. Lau, *ACS Appl. Mater. Interfaces* **2015**, *7*, 24008.
[184] S. A. More, R. G. Halor, R. Shaikh, G. G. Bisen, H. S. Tarkas, S. R. Tak, B. R. Bade, S. R. Jadkar, J. V. Sali, S. S. Ghosh, *RSC Adv.* **2020**, *10*, 39995.
[185] M. He, S. Chen, T. Wang, G. Xu, N. Liu, F. Xu, *Crystals (Basel)* **2023**, *13*, 549.
[186] Since it is very hard to quantify the amount of solvent vapor, we do not require groups to report it. However, it is highly appreciated if the estimated load and kinds of solvents, alongside the filter model are provided.
[187] A. Mhamdi, H. Mehdi, A. Bouazizi, *J. Mater. Sci.: Mater. Electron.* **2021**, *32*, 2302.
[188] VDI-Gesellschaft Verfahrenstechnik und Chemieingenieurwesen, *VDI-Wärmeatlas*, Springer Vieweg, Berlin, Heidelberg, **2013**.
[189] Y. Long, K. Liu, Y. Zhang, W. Li, *Molecules* **2021**, *26*, 3398.
[190] L. M. Falk, K. P. Goetz, V. Lami, Q. An, P. Fassl, J. Herkel, F. Thome, A. D. Taylor, F. Paulus, Y. Vaynzof, *Energy Technol (Weinh)* **2020**, *8*, 1900737.
[191] P. Fassl, V. Lami, A. Bausch, Z. Wang, M. T. Klug, H. J. Snaith, Y. Vaynzof, *Energy Environ. Sci.* **2018**, *11*, 3380.
[192] R. A. Kerner, E. D. Christensen, S. P. Harvey, J. Messinger, S. N. Habisreutinger, F. Zhang, G. E. Eperon, L. T. Schelhas, K. Zhu, J. J. Berry, D. T. Moore, *ACS Appl. Energy Mater.* **2023**, *6*, 295.
[193] Y. H. Seo, E. C. Kim, S. P. Cho, S. S. Kim, S. I. Na, *Appl. Mater. Today* **2017**, *9*, 598.
[194] S. Abicho, B. Hailegnaw, G. A. Workneh, T. Yohannes, *Materials for Renewable and Sustainable Energy* **2021**, *11*, 47.

[195] J. J. Y. W. Foong, H. A. Dewi, A. A. Zhumekenov, B. Febriansyah, A. Bruno, T. Salim, D. J. J. Tay, H. R. Abuzeid, T. M. Koh, S. G. Mhaisalkar, N. Mathews, *Sustain Energy Fuels* **2024**, *8*, 491.
[196] K. Wang, B. Yu, C. Lin, R. Yao, H. Yu, H. Wang, *Sol. RRL* **2023**, *7*, 2300137.
[197] N. J. Jeon, J. H. Noh, W. S. Yang, Y. C. Kim, S. Ryu, J. Seo, S. Il Seok, *Nature* **2015**, *517*, 476.
[198] J. Li, Y. Han, W. Jiang, P. Huang, R. Cai, M. Wang, J. Bian, *Appl. Phys. Lett.* **2023**, *122*, 013901.
[199] G. Tong, D. Y. Son, L. K. Ono, H. B. Kang, S. He, L. Qiu, H. Zhang, Y. Liu, J. Hieulle, Y. Qi, *Nano Energy* **2021**, *87*, 106152.
[200] Y. Gao, H. Raza, Z. Zhang, W. Chen, Z. Liu, Y. Gao, Z. Zhang, H. Raza, W. Chen, Z. Liu, *Adv. Funct. Mater.* **2023**, *33*, 2215171.
[201] Y. Deng, X. Zheng, Y. Bai, Q. Wang, J. Zhao, J. Huang, *Nat. Energy* **2018**, *3*, 560.
[202] A. Alasiri, K. Zubair, S. Rassel, D. Ban, O. D. Alshehri, *Heliyon* **2024**, *10*, 39141.
[203] M. Wang, W. Wang, Y. Shen, J. Ma, W. Shen, K. Cao, L. Liu, S. Chen, *ACS Appl. Mater. Interfaces* **2022**, *14*, 53960.
[204] G. Namkoong, A. A. Mamun, T. T. Ava, K. Zhang, H. Baumgart, *Org. Electron.* **2017**, *42*, 228.
[205] Q. Hu, L. Zhao, J. Wu, K. Gao, D. Luo, Y. Jiang, Z. Zhang, C. Zhu, E. Schaible, A. Hexemer, C. Wang, Y. Liu, W. Zhang, M. Grätzel, F. Liu, T. P. Russell, R. Zhu, Q. Gong, *Nat. Commun.* **2017**, *8*, 15688.
[206] D. N. Jeong, D. K. Lee, S. Seo, S. Y. Lim, Y. Zhang, H. Shin, H. Cheong, N. G. Park, *ACS Energy Lett.* **2019**, *4*, 1189.
[207] M. E. O'Kane, J. A. Smith, R. C. Kilbride, E. L. K. Spooner, C. P. Duif, T. E. Catley, A. L. Washington, S. M. King, S. R. Parnell, A. J. Parnell, *Chem. Mater.* **2022**, *34*, 7232.
[208] J. Li, J. Dagar, O. Shargaieva, M. A. Flatken, H. Köbler, M. Fenske, C. Schultz, B. Stegemann, J. Just, D. M. Többens, A. Abate, R. Munir, E. Unger, *Adv. Energy Mater.* **2021**, *11*, 2003460.
[209] P. Boonmongkolras, D. Kim, E. M. Alhabshi, I. Gereige, B. Shin, *RSC Adv.* **2018**, *8*, 21551.
[210] X. Wang, Y. Fan, L. Wang, C. Chen, Z. Li, R. Liu, H. Meng, Z. Shao, X. Du, H. Zhang, G. Cui, S. Pang, *Chem* **2020**, *6*, 1369.
[211] W. Zhang, J. Xiong, J. Li, W. A. Daoud, *Sol. RRL* **2020**, *4*, 1900370.
[212] S. Zuo, W. Niu, S. Chu, P. An, H. Huang, L. Zheng, L. Zhao, J. Zhang, *J. Phys. Chem. Lett.* **2023**, *14*, 4876.
[213] E. Radicchi, F. Ambrosio, E. Mosconi, A. A. Alasmari, F. A. S. Alasmary, F. de Angelis, *J. Phys. Chem. B* **2020**, *124*, 11481.
[214] E. J. Juarez-Perez, L. K. Ono, I. Uriarte, E. J. Cocinero, Y. Qi, *ACS Appl. Mater. Interfaces* **2019**, *11*, 12586.
[215] B. Li, Q. Dai, S. Yun, J. Tian, *J Mater Chem A Mater* **2021**, *9*, 6732.
[216] This definition does not always coincide with the colloquial use of the term 'substrate' in the laboratory, where rigid transparent conductive oxide films (TCO) such as indium tin oxide (ITO) or fluorine tin oxide (FTO) are often considered part of the substrate.
[217] H. S. Jung, G. S. Han, N. G. Park, M. J. Ko, *Joule* **2019**, *3*, 1850.
[218] X. Li, H. Yu, Z. Liu, J. Huang, X. Ma, Y. Liu, Q. Sun, L. Dai, S. Ahmad, Y. Shen, M. Wang, *Nano-Micro Lett.* **2023**, *15*, 1.
[219] L. A. Castriotta, M. A. Uddin, H. Jiao, J. Huang, *Adv. Mater.* **2025**, *37*, 2408036.
[220] W. Cai, Y. Wang, W. Li, Y. Yin, J. Liu, W. Cai, S. Wang, J. Guo, S. Chang, S. Li, X. Wang, Y. Shi, *Adv. Energy Mater.* **2024**, *14*, 2304521.
[221] We do not require these info and assume the parameter as specified if the cleaning procedure is described.
[222] the area of interest is just the extract of the thin film used for further characterization, for example a PSC's active area investigated by a JV-sweep under a solar simulator or the area investigated with a microscope.
[223] B. M. Shankar, I. S. Shivakumara, *Zeitschrift fur Angewandte Mathematik und Physik* **2021**, *72*, 1.
[224] T. Wang, T. Zhang, J. Zhang, B. Zhao, C. Song, H. Yin, S. Zhu, X. Sun, H. Liu, Y. Chen, X. Li, *J Mater Chem C Mater* **2024**, *12*, 913.
[225] T. Hou, M. Zhang, W. Yu, X. Wang, Z. Gu, Q. Chen, L. Lan, X. Sun, Y. Huang, B. Zheng, X. Liu, M. A. Green, X. Hao, *J Mater Chem A Mater* **2022**, *10*, 2105.
[226] C. J. Lawrence, *Phys. Fluids* **1988**, *31*, 2786.
[227] A. Münch, C. P. Please, B. Wagner, *Phys. Fluids* **2011**, *23*, 102101.
[228] A. G. Emslie, F. T. Bonner, L. G. Peck, *J. Appl. Phys.* **1958**, *29*, 858.
[229] S. Wang, C. Zhang, Y. Feng, Y. Shao, Y. Yan, Q. Dong, J. Liu, B. Hu, S. Jin, Y. Shi, *J Mater Chem A Mater* **2018**, *6*, 8860.
[230] H. Zhang, C. Zhao, D. Li, H. Guo, F. Liao, W. Cao, X. Niu, Y. Zhao, *J Mater Chem A Mater* **2019**, *7*, 2804.
[231] S. S. Mali, J. V. Patil, C. K. Hong, *Nano Lett.* **2019**, *19*, 6213.
[232] D. G. Lee, P. Pandey, J. Bahadur, J. T. Song, J. S. Cho, D. W. Kang, *Int. J. Energy Res.* **2024**, *2024*, 9417829.
[233] J. Kumberg, M. Baunach, J. C. Eser, A. Altvater, P. Scharfer, W. Schabel, *Energy Technol.* **2021**, *9*, 2000889.
[234] L. Tan, H. Jiang, R. Yang, L. Shen, C. Sun, Y. Jin, X. Guan, P. Song, L. Zheng, C. Tian, L. Xie, J. Yang, Z. Wei, *Adv. Energy Mater.* **2024**, *14*, 2400549.
[235] Y. Sun, Y. Zhang, Q. Liang, Y. Zhang, H. Chi, Y. Shi, D. Fang, *RSC Adv.* **2013**, *3*, 11925.
[236] J. E. Bishop, J. A. Smith, D. G. Lidzey, *ACS Appl. Mater. Interfaces* **2020**, *12*, 48237.
[237] Z. Gu, Z. Huang, C. Li, M. Li, Y. Song, *Sci. Adv.* **2018**, *4*, eaat2390.
[238] Y. Yan, Y. Yang, M. Liang, M. Abdellah, T. Pullerits, K. Zheng, Z. Liang, *Nat. Commun.* **2021**, *12*, 1.
[239] G. Wang, D. Li, H. C. Cheng, Y. Li, C. Y. Chen, A. Yin, Z. Zhao, Z. Lin, H. Wu, Q. He, M. Ding, Y. Liu, Y. Huang, X. Duan, *Sci. Adv.* **2015**, *1*, e1500613.
[240] S. S. Sangale, D. S. Mann, H. J. Lee, S. N. Kwon, S. I. Na, *Commun. Mater.* **2024**, *5*, 201.
[241] M. Pylnev, A. M. Barbisan, T. C. Wei, *Appl. Surf. Sci.* **2021**, *541*, 148559.
[242] S. Bhattacharya, A. Datta, J. M. Berg, S. Gangopadhyay, *J. Microelectromech. Syst.* **2005**, *14*, 590.
[243] J. Liu, F. Chen, H. Zheng, S. Liu, J. Sun, S. Huang, J. Song, Z. Jin, X. Liu, *RSC Adv.* **2016**, *6*, 79437.
[244] M. R. Ahmadian-Yazdi, A. Rahimzadeh, Z. Chouqi, Y. Miao, M. Eslamian, *AIP Adv.* **2018**, *8*, 25109.
[245] E. Berger, M. Bagheri, S. Asgari, J. Zhou, M. Kokkonen, P. Talebi, J. Luo, A. F. Nogueira, T. Watson, S. G. Hashmi, *Sustain Energy Fuels* **2022**, *6*, 2879.
[246] A. Giuri, E. Saleh, A. Listorti, S. Colella, A. Rizzo, C. Tuck, C. E. Corcione, *Nanomaterials* **2019**, *9*, 582.
[247] M. He, B. Li, X. Cui, B. Jiang, Y. He, Y. Chen, D. O'Neil, P. Szymanski, M. A. Ei-Sayed, J. Huang, Z. Lin, *Nat. Commun.* **2017**, *8*, 1.
[248] X. Han, B. Li, Y. Zhao, C. Tian, K. Li, C. Hou, Y. Li, H. Wang, Q. Zhang, *Sol. Energy* **2024**, *271*, 112454.
[249] J. Erz, *In-Situ Visualisierung Von Oberflächendeformationen Aufgrund von Marangoni-Konvektion Während der Filmtrocknung*, KIT Scientific Publsihing, Karlsruhe, Germany **2013**.
[250] H. Hu, R. G. Larson, *J. Phys. Chem. B* **2006**, *110*, 7090.
[251] X. Fanton, A. M. Cazabat, *Langmuir* **1998**, *14*, 2554.
[252] Q. Jiang, J. Tong, R. A. Scheidt, X. Wang, A. E. Louks, Y. Xian, R. Tirawat, A. F. Palmstrom, M. P. Hautzinger, S. P. Harvey, S. Johnston, L. T. Schelhas, B. W. Larson, E. L. Warren, M. C. Beard, J. J. Berry, Y. Yan, K. Zhu, *Science (1979)* **2022**, *378*, 1295.
[253] M. Yang, Z. Li, M. O. Reese, O. G. Reid, D. H. Kim, S. Siol, T. R. Klein, Y. Yan, J. J. Berry, M. F. A. M. van Hest, K. Zhu, *Nat. Energy* **2017**, *2*, 17038.
[254] J. C. Hamill, J. Schwartz, Y. L. Loo, *ACS Energy Lett.* **2018**, *3*, 92.

[255] S. C. Kaczaral, D. A. Morales, S. W. Schreiber, D. Martinez, A. M. Conley, R. Herath, G. E. Eperon, J. J. Choi, M. D. McGehee, D. T. Moore, D. A. Morales Jr, *APL Energy* **2023**, *1*, 036112.
[256] H. C. Weerasinghe, N. Macadam, J. E. Kim, L. J. Sutherland, D. Angmo, L. W. T. Ng, A. D. Scully, F. Glenn, R. Chantler, N. L. Chang, M. Dehghanimadvar, L. Shi, A. W. Y. Ho-Baillie, R. Egan, A. S. R. Chesman, M. Gao, J. J. Jasieniak, T. Hasan, D. Vak, *Nat. Commun.* **2024**, *15*, 1.
[257] E. Tomita, Y. Hamamoto, H. Tsutsumi, S. Yoshiyama, E. Tomita, Y. Hamamoto, H. Tsutsumi, S. Yoshiyama, *Measurement of Ambient Air Entrainment into Transient Free Gas Jet by Means of Flow Visualization*, JOURNAL OF FUELS & LUBRICANTS (1995), Vol. 104, Section 4, pp. 8-19
[258] J. Kim, L. T. Schelhas, K. H. Stone, *ACS Appl. Energy Mater.* **2020**, *3*, 11269.
[259] H. M. Hofmann, M. Kind, H. Martin, *Int J Heat Mass Transf* **2007**, *50*, 3957.
[260] J. H. Lienhard, 18th National & 7th ISHMT-ASME Heat and Mass Transfer Conference **2005**.
[261] L. L. Gao, C. X. Li, C. J. Li, G. J. Yang, *J Mater Chem A Mater* **2017**, *5*, 1548.
[262] "ISO 8655-1:2022 – Appareils volumétriques à piston — Partie 1: Définitions, exigences générales et recommandations pour l'utilisateur", can be found under, https://www.iso.org/fr/standard/68796.html (accessed: June 2024).
[263] We are still lenient with specifying the nozzle opening and accept the volume antisolvent as an equivalent parameter in Section 4. This should however not be seen as an incentive to do so.
[264] D.-T. Chin, M. Agarwal, *J. Electrochem. Soc.* **1991**, *138*, 2643.
[265] A. D. Taylor, Q. Sun, K. P. Goetz, Q. An, T. Schramm, Y. Hofstetter, M. Litterst, F. Paulus, Y. Vaynzof, *Nat. Commun.* **2021**, *12*, 1878.
[266] A. Babayigit, J. D'Haen, H. G. Boyen, B. Conings, *Joule* **2018**, *2*, 1205.
[267] In an analogy well-established in electrical engineering, one could argue that, in a circuit of unknown electrical devices connected in series, the voltage (that is the pressure) with respect to ground at a certain point in the circuit does not contain a lot of information. However, the total current (that is the gas flow rate) does contain more information because it is conserved everywhere in the circuit.
[268] B. Yan, W. Dai, Z. Wang, Z. Zhong, L. Zhang, M. Yu, Q. Zhou, Q. Ma, K. Yan, L. Zhang, Y. M. Yang, J. Yao, *Science* **2025**, *388*, adt5001.
[269] L. Gao, K. Zhang,N. Chen, G. Yang, Journal of Materials Chemistry A, 2017, 5, 18120.
[270] H. H. Huang, Q. H. Liu, H. Tsai, S. Shrestha, L. Y. Su, P. T. Chen, Y. T. Chen, T. A. Yang, H. Lu, C. H. Chuang, K. F. Lin, S. P. Rwei, W. Nie, L. Wang, *Joule* **2021**, *5*, 958.
[271] From the perspective of heat and mass transfer, the distinction between the two methods is often not very sharp as infrared radiation (alongside convective and conductive heat transfer) is generated by all heated surfaces.
[272] N. Rolston, W. J. Scheideler, A. C. Flick, J. P. Chen, H. Elmaraghi, A. Sleugh, O. Zhao, M. Woodhouse, R. H. Dauskardt, *Joule* **2020**, *4*, 2675.
[273] This type of radiation is also emitted from hotplates and ovens.
[274] S. Chen, X. Xiao, B. Chen, L. L. Kelly, J. Zhao, Y. Lin, M. F. Toney, J. Huang, *Sci. Adv.* **2021**, *7*, eabb2412.
[275] T. Du, S. R. Ratnasingham, F. U. Kosasih, T. J. Macdonald, L. Mohan, A. Augurio, H. Ahli, C. T. Lin, S. Xu, W. Xu, R. Binions, C. Ducati, J. R. Durrant, J. Briscoe, M. A. McLachlan, *Adv. Energy Mater.* **2021**, *11*, 2101420.
[276] S. R. Ratnasingham, L. Mohan, M. Daboczi, T. Degousée, R. Binions, O. Fenwick, J. S. Kim, M. A. McLachlan, J. Briscoe, *Mater. Adv.* **2021**, *2*, 1606.
[277] J. Wu, X. Xu, Y. Zhao, J. Shi, Y. Xu, Y. Luo, D. Li, H. Wu, Q. Meng, *ACS Appl. Mater. Interfaces* **2017**, *9*, 26937.
[278] T. Liu, Q. Hu, J. Wu, K. Chen, L. Zhao, F. Liu, C. Wang, H. Lu, S. Jia, T. Russell, R. Zhu, Q. Gong, *Adv. Energy Mater.* **2016**, *6*, 1501890.
[279] Z. Xiao, C. Bi, Y. Shao, Q. Dong, Q. Wang, Y. Yuan, C. Wang, Y. Gao, J. Huang, *Energy Environ. Sci.* **2014**, *7*, 2619.
[280] Y. Jo, K. Suk Oh, M. Kim, K.-H. Kim, H. Lee, C.-W. Lee, D. Suk Kim, Y. Jo, K. S. Oh, M. Kim, K. Kim, D. S. Kim, H. Lee, C. Lee, *Adv. Mater. Interfaces* **2016**, *3*, 1500768.
[281] M. Sun, C. Liang, H. Zhang, C. Ji, F. Sun, F. You, X. Jing, Z. He, *J Mater Chem A Mater* **2018**, *6*, 24793.
[282] S. Li, H. Ren, Y. Yan, *Appl. Surf. Sci.* **2019**, *484*, 1191.
[283] Q. Jiang, Z. Chu, P. Wang, X. Yang, H. Liu, Y. Wang, Z. Yin, J. Wu, X. Zhang, J. You, Q. Jiang, Z. Chu, P. Wang, X. Yang, H. Liu, Y. Wang, Z. Yin, J. Wu, X. Zhang, J. You, *Adv. Mater.* **2017**, *29*, 1703852.
[284] Y. Zhao, Q. Li, W. Zhou, Y. Hou, Y. Zhao, R. Fu, D. Yu, X. Liu, Q. Zhao, *Sol. RRL* **2019**, *3*, 1800296.
[285] J. H. Lee, K. Jung, M. J. Lee, *J. Alloys Compd.* **2021**, *879*, 160373.
[286] K. Jung, M. J. Lee, *Mater. Lett.* **2021**, *292*, 129623.
[287] M. A. Mahmud, N. K. Elumalai, M. B. Upama, D. Wang, B. Puthen-Veettil, F. Haque, M. Wright, C. Xu, A. Pivrikas, A. Uddin, *Sol. Energy Mater. Sol. Cells* **2017**, *167*, 87.
[288] T. Vetter, M. Iggland, D. R. Ochsenbein, F. S. Hänseler, M. Mazzotti, *Cryst. Growth Des.* **2013**, *13*, 4890.
[289] V. O. Eze, Y. Seike, T. Mori, *ACS Appl. Mater. Interfaces* **2020**, *12*, 46837.
[290] M. Kim, G. H. Kim, T. K. Lee, I. W. Choi, H. W. Choi, Y. Jo, Y. J. Yoon, J. W. Kim, J. Lee, D. Huh, H. Lee, S. K. Kwak, J. Y. Kim, D. S. Kim, *Joule* **2019**, *3*, 2179.
[291] L. Zhu, H. Cao, C. Xue, H. Zhang, M. Qin, J. Wang, K. Wen, Z. Fu, T. Jiang, L. Xu, Y. Zhang, Y. Cao, C. Tu, J. Zhang, D. Liu, G. Zhang, D. Kong, N. Fan, G. Li, C. Yi, Q. Peng, J. Chang, X. Lu, N. Wang, W. Huang, J. Wang, *Nat. Commun.* **2021**, *12*, 1.
[292] W. Qiu, T. Merckx, M. Jaysankar, C. Masse De La Huerta, L. Rakocevic, W. Zhang, U. W. Paetzold, R. Gehlhaar, L. Froyen, J. Poortmans, D. Cheyns, H. J. Snaith, P. Heremans, *Energy Environ. Sci.* **2016**, *9*, 484.
[293] A. Farooq, I. M. Hossain, S. Moghadamzadeh, J. A. Schwenzer, T. Abzieher, B. S. Richards, E. Klampaftis, U. W. Paetzold, *ACS Appl. Mater. Interfaces* **2018**, *10*, 21985.
[294] Y. Yao, X. Zou, J. Cheng, D. Chen, C. Chang, T. Ling, H. Ren, *Crystals* **2019**, *9*, 151.
[295] L. Tian, W. Zhang, Y. Huang, F. Wen, H. Yu, Y. Li, Q. Wang, C. Peng, Z. Ma, T. Hu, L. Du, M. Zhang, *ACS Appl. Mater. Interfaces* **2020**, *12*, 29344.
[296] A. A. Qureshi, S. Javed, M. Adnan, M. Jamshaid, M. Aftab Akram, U. Ali, *ChemistrySelect* **2023**, *8*, 202300342.
[297] S. Abbasi, X. Wang, P. Tipparak, C. Bhoomanee, P. Ruankham, H. Liu, D. Wongratanaphisan, W. Shen, *Mater. Sci. Semicond. Process.* **2023**, *155*, 107241.
[298] Y. Li, L. Meng, Y. Yang, G. Xu, Z. Hong, Q. Chen, J. You, G. Li, Y. Yang, Y. Li, *Nat. Commun.* **2016**, *7*, 1.
[299] V. L. Pool, B. Dou, D. G. Van Campen, T. R. Klein-Stockert, F. S. Barnes, S. E. Shaheen, M. I. Ahmad, M. F. A. M. Van Hest, M. F. Toney, *Nat. Commun.* **2017**, *8*, 14075.
[300] M. Alsari, O. Bikondoa, J. Bishop, M. Abdi-Jalebi, L. Y. Ozer, M. Hampton, P. Thompson, M. T. Hörantner, S. Mahesh, C. Greenland, J. E. Macdonald, G. Palmisano, H. J. Snaith, D. G. Lidzey, S. D. Stranks, R. H. Friend, S. Lilliu, *Energy Environ. Sci.* **2018**, *11*, 383.
[301] D. P. Nenon, J. A. Christians, L. M. Wheeler, J. L. Blackburn, E. M. Sanehira, B. Dou, M. L. Olsen, K. Zhu, J. J. Berry, J. M. Luther, *Energy Environ. Sci.* **2016**, *9*, 2072.
[302] H. Mehdi, A. Mhamdi, A. Bouazizi, *Physica E Low Dimens Syst Nanostruct* **2020**, *119*, 114000.

[303] M. Ali Akhavan Kazemi, A. Jamali, F. Sauvage, *Front. Energy Res.* **2021**, *9*, 732886.
[304] D. O. Oyewole, R. K. Koech, R. Ichwani, R. Ahmed, J. Hinostroza Tamayo, S. A. Adeniji, J. Cromwell, E. Colin Ulloa, O. K. Oyewole, B. Agyei-Tuffour, L. V. Titova, N. A. Burnham, W. O. Soboyejo, *AIP Adv.* **2021**, *11*, 65327.
[305] T. D. Malevu, B. S. Mwankemwa, K. G. Tshabalala, R. O. Ocaya, *Sci Afr* **2020**, *8*, 00447.
[306] S. Wu, C. Li, S. Y. Lien, P. Gao, *Chemistry* **2024**, *6*, 207.
[307] M. Kim, G. H. Kim, K. S. Oh, Y. Jo, H. Yoon, K. H. Kim, H. Lee, J. Y. Kim, D. S. Kim, *ACS Nano* **2017**, *11*, 6057.
[308] O. V. Oyelade, O. K. Oyewole, Y. A. Olanrewaju, R. Ichwani, R. Koech, D. O. Oyewole, S. A. Adeniji, D. M. Sanni, J. Cromwell, R. A. Ahmed, K. Orisekeh, V. C. Anye, W. O. Soboyejo, *AIP Adv.* **2022**, *12*, 25104.
[309] D. R. Wargulski, K. Xu, H. Hempel, M. A. Flatken, S. Albrecht, D. Abou-Ras, *ACS Appl. Mater. Interfaces* **2023**, *15*, 41516.
[310] Q. Zhou, Z. Jin, H. Li, J. Wang, *Sci. Rep.* **2016**, *6*, 1.
[311] S. R. Raga, M. C. Jung, M. V. Lee, M. R. Leyden, Y. Kato, Y. Qi, *Chem. Mater.* **2015**, *27*, 1597.
[312] I. Mesquita, L. Andrade, A. Mendes, *Sol. Energy* **2020**, *199*, 474.
[313] we count the volume of antisolvent as a nozzle size parameter in a conservative estimation. If the analysis was less lenient, the frequency of "Nozzle size" would be much lower.

Simon Ternes is a post-doctoral researcher at University of Rome Tor Vergata and CNR-ISM. His work focuses on in situ characterization and advanced modelling concepts for enhancing process control of large-scale perovskite coating. In particular, he is interested in non-invasive, rapid optical characterization techniques such as reflectance, absorption and photoluminescence for developing data-intensive models of perovskite drying and crystallization processes.

Alessio Gagliardi develops numerical models to simulate nanostructured devices, focusing on next-generation solar cells, electrochemical systems, and organic semiconductors. His multiscale expertise spans from DFT and quantum methods to Kinetic Monte Carlo and continuum models. He contributes to Tiber CAD and GDFTB software and integrates machine learning into multiscale material modeling. Gagliardi earned his engineering degree in Rome and a Ph.D. in physics from Paderborn in 2007, followed by postdoctoral research in Bremen and Rome. He joined TUM in 2014 as a Tenure Track Assistant Professor and has been an Associate Professor since 2020.

Aldo Di Carlo is a full Professor at the University of Rome Tor Vergata, Director of CNR-ISM, and President of the CNR Research Area Rome–RM2. He founded and led the Center for Hybrid and Organic Solar Energy (CHOSE) from 2006 to 2019, involving 60+ researchers in photovoltaics. He chaired the Scientific Council of the Dyepower consortium, advancing Dye Solar Cells (DSCs). His research focuses on electronic and optoelectronic devices, especially DSCs and Perovskite Solar Cells. Di Carlo has (co-)authored over 700 publications, 13 international patents, and coordinated or co-coordinated 25+ major EU projects.